

000 BETTER, FASTER: HARNESSING SELF-IMPROVEMENT 001 002 IN LARGE REASONING MODELS 003 004

005 **Anonymous authors**

006 Paper under double-blind review

007 008 ABSTRACT 009

010 While large reasoning models (LRMs) trained with explicit reasoning trajectories
011 have demonstrated impressive performance, obtaining high-quality trajectories
012 is often costly and time-consuming. Hence, recent literature introduces a
013 *self-improvement* paradigm that enables LRMs to improve themselves by self-
014 generating reasoning trajectories as training data without external supervision.
015 However, we find that this method often falls short in complex reasoning tasks
016 and even leads to model collapse. Through a series of preliminary analyses, we
017 reveal two shortcomings of self-improvement in LRMs: (1) *data imbalance*, where
018 most training samples are simple, but the challenging yet crucial samples are
019 scarce; (2) *overthinking*, where many undesired samples with redundant and repet-
020 itive reasoning steps are used for self-training. To this end, we propose **HSIR**,
021 which effectively **H**arnesses **S**elf-**I**mprovement in large **R**easoning models via two
022 simple-yet-effective approaches. Specifically, HSIR introduces a *verify-then-exit*
023 sampling strategy to mitigate data imbalance by efficiently collecting more accurate
024 solutions for difficult queries, and designs an *Intrinsic Diversity* score to quantify
025 overthinking and filter out the undesired solutions. We apply HSIR to various
026 post-training paradigms, among which we further propose H-GRPO, an enhanced
027 GRPO algorithm that leverages the intrinsic diversity as an external reward to
028 encourage concise and diverse reasoning via reinforcement learning. Extensive re-
029 sults show that HSIR not only effectively enhances the reasoning performance, *i.e.*,
030 bringing up to **+10.9%** average performance gains, but also significantly improves
031 the reasoning efficiency by reducing up to **42.4%** relative inference overhead.

032 1 INTRODUCTION

033 Recently, post-training the large language models (LLMs) with explicit long chain-of-thought (CoT)
034 reasoning trajectories has garnered significant attention (Li et al., 2025; Plaat et al., 2024; Xu et al.,
035 2025). Owing to the scaling inference compute of long-CoT reasoning, large reasoning models
036 (LRMs) can unleash their reasoning capabilities (*e.g.*, backtracking and self-correction) and achieve
037 better performance in various reasoning tasks, such as mathematical reasoning (Shao et al., 2024)
038 and medical reasoning (Chen et al., 2024c). However, the performance of LRMs highly relies on
039 high-quality intermediate reasoning trajectories (Yang et al., 2025c), which are usually costly and
040 time-consuming to obtain (Peng et al., 2025). In response to this issue, the “*self-improvement*”
041 paradigm has emerged, *i.e.*, models iteratively improve themselves by using the self-generated
042 reasoning trajectories as training data, thereby reducing their dependence on external supervision.

043 In the context of LRMs, several self-improvement approaches have been proposed to achieve better
044 reasoning performance, such as STaR (Zelikman et al., 2022) and REST^{EM} (Singh et al., 2023). For
045 instance, ReST^{EM} first prompts the model to generate multiple reasoning paths for each question,
046 then filters out the incorrect solutions, and finally fine-tunes the model using its own correct outputs.
047 These methods can boost LRMs’ performance on conventional reasoning tasks without external
048 supervision. However, in our preliminary experiments (Figure 1), we found that they often fall
049 short in complex reasoning tasks, *e.g.*, medical question-answering that requires the integration
050 of specialized knowledge with detailed patient histories and comorbidities (Huang et al., 2025b).
051 More seriously, they might suffer from *model collapse*, where models’ performance degrades due
052 to iterative self-training on model-generated data (Bertrand et al., 2024; Gerstgrasser et al., 2024).
053 Through a series of analyses (§2.2), we reveal that these methods have two major shortcomings:

054 ❶ **data imbalance**, *i.e.*, most training samples are relatively simple, whereas challenging yet crucial
 055 samples are scarce; ❷ **overthinking**, *i.e.*, many undesired solutions with redundant and repetitive
 056 reasoning steps are used for self-training, hindering models’ accurate and concise reasoning.
 057

058 Several prior studies also recognize these shortcomings and attempt to address them. Specifically,
 059 an intuitive way to mitigate data imbalance is to collect more correct solutions for difficult
 060 queries. To achieve it, Tong et al. (2024) propose to allocate more trials to difficult queries
 061 and Ding et al. (2025) leverage additional signals (*e.g.*, answers) to guide the reasoning of
 062 LRMs. Although effective, they mainly rely on increased inference overhead to obtain new solu-
 063 tions, while overlooking the potential value of previously failed solutions. On the other hand,
 064 to alleviate overthinking, the key lies in quantifying the redundancy and repetitiveness of reason-
 065 ing steps. Most existing works involve designing length-oriented metrics and simply regard
 066 shorter correct solutions as superior (Team et al., 2025; Munkhbat et al., 2025). While achieving
 067 remarkable reasoning efficiency, overly emphasizing length reduction may hinder models’ deep
 068 reasoning and lead to performance degradation (Dai et al., 2025). Thus, there arises a question: *can*
 069 *we explore a more effective self-improvement training method to make LRM*s *both better and faster?*
 070

071 To achieve this goal, we propose **HSIR**, which effectively **Harnesses Self-Improvement** in large
 072 **Reasoning** models via two simple-yet-effective approaches. First, to collect more correct responses
 073 for difficult queries, HSIR introduces a *verify-then-exit* (denoted as *VeriExit*) sampling strategy,
 074 which verifies the correctness of intermediate reasoning steps in the previously failed solution and
 075 self-truncates the reasoning once the current step arrives at the ground-truth answer. The motivation
 076 of *VeriExit* is that, within the failed solution, LRM may have arrived at the correct answer during
 077 intermediate reasoning steps, yet ultimately failed to produce the accurate outcome due to reasoning
 078 deviation. Second, motivated by the intuition that a high similarity among intermediate reasoning steps
 079 often signals redundant or repetitive thinking, HSIR designs an **Intrinsic Diversity** score (denoted as
 080 *InDiv*) to quantify overthinking using the internal states of LRM. In practice, *InDiv* performs an
 081 attention-aware eigenvalue analysis on the hidden representations of intermediate reasoning steps,
 082 where those with smaller eigenvalues are repetitive. Overall, by efficiently collecting more correct
 083 solutions and filtering out undesired overthinking solutions, HSIR can ensure the diversity and
 084 conciseness of training data, thus achieving better reasoning performance and efficiency.
 085

086 We apply our HSIR to two iterative post-training paradigms: supervised fine-tuning (SFT) and
 087 preference learning. Extensive results on seven cutting-edge LLMs and two representative reasoning
 088 tasks, *i.e.*, medical reasoning and mathematical reasoning, show that our HSIR not only outperforms
 089 the other counterparts by a clear margin, but also effectively improves the reasoning efficiency.
 090 Furthermore, we expand our methods to the currently popular Reinforcement Learning from Veri-
 091 fiable Rewards (RLVR) training paradigm (Guo et al., 2025), and propose **H-GRPO**, an enhanced
 092 GRPO (Shao et al., 2024) algorithm that leverages the *InDiv* scores as an external reward to smoothly
 093 alleviate the overthinking. More comparative results prove the superiority of H-GRPO. Additionally,
 094 more in-depth analyses prove the effectiveness of HSIR’s important components, and indicate that
 095 HSIR brings better model generalization. To summarize, our contributions are as follows:
 096

- 100 • We reveal two major shortcomings of self-improvement in LRM, and propose HSIR that leverages
 101 two simple-yet-effective approaches to alleviate them and make LRM both better and faster.
- 102 • HSIR can be adopted to various post-training paradigms. Among which, we further expand it to
 103 the popular RLVR training paradigm, and propose H-GRPO that improves the GRPO by using our
 104 proposed *InDiv* scores as an external reward to encourage LRM’s diverse and concise reasoning.
- 105 • Extensive results show that HSIR can consistently and significantly improve the reasoning perfor-
 106 mance and efficiency for a diversity of LLMs, bringing up to **+10.9%** average performance gains
 107 and reducing up to **42.4%** relative inference overhead against the initial reasoning models.

108

2 RETHINKING SELF-IMPROVEMENT TRAINING IN LRMs

109

2.1 PRELIMINARIES

110 Considering that we have a base LLM \mathcal{M}_{base} , a small amount of seed data $\mathcal{S} = \{(x_i, r_i, y_i)\}_{i=1}^N$ and
 111 a larger unlabeled dataset $\mathcal{D} = \{(x_i, y_i)\}_{i=1}^M$ ($M \gg N$), where x_i is the query, $r_i = [r_{i,1}, \dots, r_{i,L}]$
 112 is the corresponding reasoning trajectory with L intermediate steps, and y_i is the ground-truth answer.
 113 We first fine-tune \mathcal{M}_{base} on \mathcal{S} to make it have basic long-CoT reasoning ability, and denote the tuned
 114 model as \mathcal{M}_0 . The goal of self-improvement is to enhance the reasoning performance of \mathcal{M}_0 by
 115 iteratively self-training using its own solutions on \mathcal{D} over T cycles. Specifically, let \mathcal{M}_t denote the
 116 model at the t -th iteration ($t \in [1, T]$), the self-improvement training involves the following steps:
 117

118 **Self-generation.** At t -th iteration, for each query $x_i \in \mathcal{D}$, we enforce the previous model \mathcal{M}_{t-1}
 119 to generate multiple reasoning trajectories and their corresponding answers $\{(\hat{r}_i^k, \hat{y}_i^k)\}_{k=1}^K$, where
 120 $k \in [1, K]$ and K denotes the total sampling times for each query. By doing so, we can obtain the
 121 self-generated dataset $\hat{\mathcal{D}}_t = \{(x_i, \hat{r}_i^k, \hat{y}_i^k) \mid x_i \in \mathcal{D}; k \in [1, K]\}$.
 122

123 **Self-training.** The self-training process differs across various post-training paradigms. Specifically,
 124 during **SFT** training, the ground-truth answer y_i is used to verify the correctness of candidate solutions
 125 $\{(\hat{r}_i^k, \hat{y}_i^k)\}_{k=1}^K$, where only correct solutions with $\mathbb{I}(\hat{y}_i^k, y_i) = 1$ are filtered to form the pseudo-labeled
 126 dataset $\hat{\mathcal{D}}_t^{correct} = \{(x_i, \hat{r}_i^k, \hat{y}_i^k) \mid x_i \in \mathcal{D}; k \in [1, K]; \mathbb{I}(\hat{y}_i^k, y_i) = 1\}$. Notably, to alleviate the
 127 model collapse problem, we follow the prior studies (Alemohammad et al., 2024; Wang et al., 2024)
 128 and use the combination of the original clean seed dataset \mathcal{S} and the pseudo-labeled dataset $\hat{\mathcal{D}}_t^{correct}$
 129 as the final training dataset $\mathcal{D}_t = \mathcal{S} \cup \hat{\mathcal{D}}_t^{correct}$. Considering that continually fine-tuning \mathcal{M}_{t-1} would
 130 lead to overfitting, we fine-tune the base model \mathcal{M}_{base} on \mathcal{D}_t to obtain the new model \mathcal{M}_t , following
 131 previous practice (Zelikman et al., 2022; Singh et al., 2023). In particular, we optimize \mathcal{M}_t using the
 132 standard negative log likelihood (NLL) loss function:
 133

$$134 \mathcal{L}_{SFT} = \mathbb{E}_{\mathcal{D}_t} \left[-\log \frac{\mathcal{M}_\theta(\hat{r}_i^k, \hat{y}_i^k | x_i)}{|\hat{r}_i^k| + |\hat{y}_i^k|} \right], \quad (1)$$

135 where \mathcal{M}_θ initialized with \mathcal{M}_{base} denotes the current tuned model that will become next model \mathcal{M}_t .
 136

137 For the implementation of **preference learning**, we utilize a representative and effective algorithm,
 138 *i.e.*, Direct Preference Optimization (DPO) (Rafailov et al., 2023). Specifically, for each query $x_i \in$
 139 $\hat{\mathcal{D}}_t$, we split the candidate solutions into two sets: winner $\{(x_i, \hat{r}_i^{k_w}, \hat{y}_i^{k_w}) \mid \mathbb{I}(\hat{y}_i^{k_w}, y_i) = 1\}$ and loser
 140 $\{(x_i, \hat{r}_i^{k_l}, \hat{y}_i^{k_l}) \mid \mathbb{I}(\hat{y}_i^{k_l}, y_i) = 0\}$. Then, each winning solution and a randomly-selected losing solution
 141 are paired to construct the preference training set $\hat{\mathcal{D}}_t^{pairs} = \{(x_i, \hat{r}_i^{k_w}, \hat{y}_i^{k_w}), (x_i, \hat{r}_i^{k_l}, \hat{y}_i^{k_l}) \mid x_i \in$
 142 $\hat{\mathcal{D}}_t; k_w, k_l \in [1, K]\}$. Lastly, we can obtain the new model \mathcal{M}_t by continually optimizing \mathcal{M}_{t-1}
 143 on $\hat{\mathcal{D}}_t^{pairs}$. Inspired by Pang et al. (2024), we employ an enhanced DPO algorithm that combines
 144 the standard DPO loss function and NLL loss function on winning solutions to ensure the training
 145 stability, which is formulated as follows:
 146

$$147 \mathcal{L}_{DPO+NLL} = \mathcal{L}_{DPO}(\hat{r}_i^{k_w}, \hat{y}_i^{k_w}, \hat{r}_i^{k_l}, \hat{y}_i^{k_l} | x_i) + \alpha_{nll} \cdot \mathcal{L}_{NLL}(\hat{r}_i^{k_w}, \hat{y}_i^{k_w} | x_i) \\ 148 = \mathbb{E}_{\hat{\mathcal{D}}_t^{pairs}} \left[-\log \sigma \left(f(\hat{r}_i^{k_w}, \hat{y}_i^{k_w} | x_i) - f(\hat{r}_i^{k_l}, \hat{y}_i^{k_l} | x_i) \right) - \alpha_{nll} \cdot \frac{\log \mathcal{M}_\theta(\hat{r}_i^{k_w}, \hat{y}_i^{k_w} | x_i)}{|\hat{r}_i^{k_w}| + |\hat{y}_i^{k_w}|} \right], \quad (2)$$

149 where σ is the sigmoid function, $f(\cdot | x_i) = \beta \log \frac{\mathcal{M}_\theta(\cdot | x_i)}{\mathcal{M}_{t-1}(\cdot | x_i)}$, \mathcal{M}_θ is the policy model initialized with
 150 \mathcal{M}_{t-1} , α_{nll} and β are coefficients that are empirically set to 0.5 and 0.1, respectively. Finally, we
 151 can obtain our next model \mathcal{M}_t , which will be used to generate data for the subsequent iteration.
 152

153

2.2 EMPIRICAL ANALYSES

154 **Settings.** We conduct preliminary experiments by fine-tuning Qwen2.5-1.5B/3B/7B instruct
 155 models (Yang et al., 2024) on a challenging medical reasoning dataset, *i.e.*, MedQA (Jin et al., 2021).
 156 Specifically, since the original MedQA training set does not contain any reasoning trajectories, we
 157 prompt the proprietary DeepSeek-R1 to generate the seed reasoning data. By filtering out incorrect
 158 solutions, we ultimately obtained a new training set containing 9.3K reasoning samples. From this

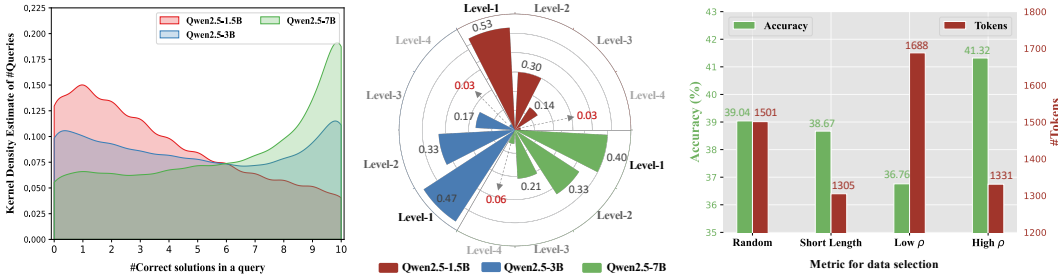


Figure 2: **Left:** Distribution of the number of correct solutions in a single query. **Middle:** Distribution of self-generated training samples with different difficulty levels, where level-1 means the simplest and level-4 means the most difficult. **Right:** Performance comparison between tuned Qwen2.5-1.5B models using different data selection methods. Here, all experiments are based on the MedQA task.

set, we randomly selected 1K as seed data \mathcal{S} , while treating the remaining samples as unlabeled data \mathcal{D} (*i.e.*, without using their reasoning trajectories). For the implementation of self-improvement training, the number of iterations T is set to 1, and the total sampling times K is set to 10. **Notably, $T = 1$ means that we perform the self-improvement training for one iteration, *i.e.*, from \mathcal{M}_0 to \mathcal{M}_1 .**

Findings. Through extensive analyses on the self-generated training samples, we found that there are two major problems: data imbalance and overthinking. Specifically,

① Data Imbalance: Figure 2 (Left) illustrates the distribution of the number of correct solutions in a query. As seen, there is a positive correlation between the number of correct solutions and model capabilities, where stronger models (*e.g.*, Qwen2.5-7B) can collect more accurate solutions for each query. However, for the difficult queries that are proven to be more crucial for further training (Liu et al., 2024), these models still struggle to collect sufficient correct solutions, thus leading to data imbalance. Specifically, although for the powerful Qwen2.5-7B, there are more than 500 queries that did not obtain any correct solutions. To have a close look, based on the number of correct solutions in a query, we evenly split the queries into four levels, where level-1 refers to the simplest queries obtaining the most correct solutions, and level-4 refers to the most difficult queries. Figure 2 (Middle) shows the distribution of self-generated training samples at different levels, indicating that **most training samples are relatively simple, whereas challenging yet crucial samples are scarce**.

② Overthinking: As a common issue in LRMs, overthinking usually leads to inefficient reasoning and suboptimal performance (Chen et al., 2024d). The key to alleviating overthinking lies in quantifying it via a fair and accurate metric. Motivated by the intuition that a high similarity among intermediate reasoning steps often indicates redundant or repetitive thinking, we introduce a **reasoning diversity metric** to measure the diversity of reasoning steps. As shown in Algorithm 1, for each reasoning trajectory \hat{r}_i^k , we first convert all intermediate reasoning steps $[\hat{r}_{i,1}^k, \dots, \hat{r}_{i,L}^k]$ into sentence embeddings using the BGE-m3 model (Chen et al., 2024b), and then calculate the cosine distance between $\hat{r}_{i,l}^k$ and its nearest neighbor in the current subset. The reasoning steps with cosine distance below the threshold τ_{sim} are regarded as repetitive and are filtered out. The τ_{sim} is empirically set to 0.85 in our work. The metric ρ is defined as the ratio of unfiltered steps to all steps:

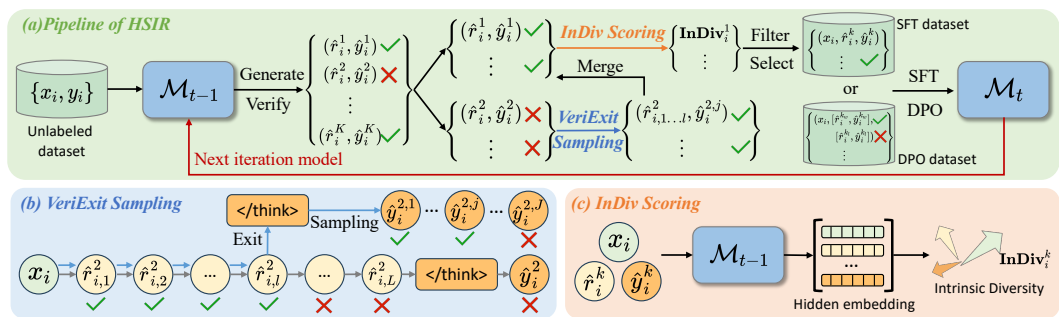
$$\rho_i^k = \frac{|\mathcal{U}(\hat{r}_i^k)|}{|[\hat{r}_{i,1}^k, \dots, \hat{r}_{i,L}^k]|}, \quad \rho_i^k \in (0, 1] \quad (3)$$

where $\mathcal{U}(\cdot)$ denotes the set of unfiltered steps. To verify the effectiveness of this metric, we conduct comparative experiments by using the solution with the highest and lowest ρ_i^k for each query as self-training data, respectively. For reference, we also employ a random and a length-penalty method as baselines, *i.e.*, using a randomly selected solution and the shortest solution for self-training, respectively. Figure 2 (Right) shows the comparative results of Qwen2.5-1.5B models on the MedQA test set, using the average accuracy and number of output tokens as metrics. As seen, compared to using random solutions, self-training on solutions with low ρ scores indeed results in more inference overhead and lower accuracy, while using the solutions with high ρ scores can effectively alleviate this problem. Notably, although self-training on shorter solutions is also beneficial to improve reasoning efficiency, it would lead to performance degradation. These results suggest that **self-training with redundant and repetitive reasoning steps undermines the accuracy and conciseness of models’ reasoning**, which is difficult to resolve effectively through length-penalty methods alone.

216 3 HARNESS SELF-IMPROVEMENT FOR BETTER AND FASTER REASONING

217 3.1 MOTIVATION AND INTUITION OF HSIR

218 To alleviate the above problems, we propose HSIR that harnesses self-improvement in LRM_s via two
 219 simple-yet-effective approaches. First, to address data imbalance, we build upon the insight (Yang
 220 et al., 2025b; Dai et al., 2025) that failed solutions are not entirely incorrect but often contain valuable,
 221 partially correct reasoning steps before deviating. Instead of discarding these outputs, we introduce
 222 **VeriExit**, a novel **trajectory recycling** strategy. It efficiently salvages valid initial reasoning from
 223 failed attempts to generate correct solutions for difficult queries. This approach provides a significant
 224 efficiency gain over costly resampling from scratch. Second, to combat overthinking, our empirical
 225 analysis in §2.2 validates that reasoning diversity is a potent signal, yet the preliminary metric (Eq. 3)
 226 relies on costly external models. We propose a more elegant solution by harnessing the dense semantic
 227 information already present in a model’s internal states. We introduce the **Intrinsic Diversity (InDiv)**
 228 **score**, an efficient metric that measures diversity directly from the models’ hidden representations.
 229 This makes *InDiv* an **entirely intrinsic** measure that eliminates external dependencies and can be
 230 computed with minimal to zero overhead. Figure 3 illustrates the overview of our HSIR.
 231



232 Figure 3: (a) Pipeline of self-improvement training with HSIR. After generating candidate solutions
 233 for each query, we first employ our (b) VeriExit sampling strategy to collect more accurate solutions
 234 for difficult queries, and then quantify the overthinking of correct solutions via our (c) *InDiv*.
 235 Lastly, the accurate, diverse, and concise solutions are selected for iterative SFT/DPO training.
 236

237 3.2 IMPORTANT COMPONENTS OF HSIR

238 **Verify-then-Exit Decoding Strategy.** After obtaining the self-generated dataset $\hat{\mathcal{D}}_t$, we select
 239 the incorrect solutions from it to form a new set $\hat{\mathcal{D}}_t^{wrong} = \{(x_i, \hat{r}_i^k, \hat{y}_i^k) | x_i \in \mathcal{D}; \mathbb{I}(\hat{y}_i^k, y_i) = 0\}$.
 240 For each $\hat{r}_i^k \in \hat{\mathcal{D}}_t^{wrong}$, we verify the correctness of intermediate reasoning steps $[\hat{r}_{i,1}^k, \dots, \hat{r}_{i,L}^k]$
 241 by determining whether the $\hat{r}_{i,l}^k$ ($l \in [1, L]$) arrives at the ground-truth answer y_i ¹, e.g., explicitly
 242 mentioning “answer is $\{y_i\}$ ”. Once $\hat{r}_{i,l}^k$ arrives at y_i , we truncate the subsequent reasoning steps
 243 and insert the exit prompt “`\n\n</think>\n<answer>\n`” at the truncated position. That is,
 244 we can obtain a new query “ $x_i + [\hat{r}_{i,1}^k, \dots, \hat{r}_{i,l}^k] + \text{exit prompt} + \dots + \hat{y}_i^k$ ”, which is
 245 then fed into \mathcal{M}_{t-1} to stop further reasoning and produce answers. Moreover, to ensure that \mathcal{M}_{t-1}
 246 can output the correct answers, we sample J times and collect the correct solutions $\hat{\mathcal{D}}_t^{VeriExit} =$
 247 $\{(x_i, \hat{r}_{i,1}^k, \hat{y}_i^{k,j}) | \mathbb{I}(\hat{y}_i^{k,j}, y_i) = 1; k \in [1, K]; j \in [1, J]\}$. Notably, $J < K$, and such a sampling
 248 process will not lead to much inference overhead, compared to resampling the complete reasoning
 249 trajectories. Lastly, the $\hat{\mathcal{D}}_t^{VeriExit}$ is merged into the original correct solutions $\hat{\mathcal{D}}_t^{correct}$. If the
 250 total number of correct solutions for x_i is larger than K , we randomly sample K ones to maintain
 251 consistency between the training budgets of our method and vanilla self-improvement methods.
 252

253 **Intrinsic Diversity Score.** To quantify overthinking, we leverage the LLMs’ internal states to
 254 measure the semantic diversity of reasoning steps. Specifically, for each correct solution $(x_i, \hat{r}_i^k, \hat{y}_i^k)$,
 255 we obtain its hidden representation $\mathbf{H}_i^k \in \mathbb{R}^{d \times m}$ at the middle layer of \mathcal{M}_{t-1} , where d is the
 256 dimension of hidden states and m is the number of all tokens in the solution. We choose the middle
 257

258 ¹There are several ways to achieve this, e.g., text-matching, NLI-based and prompt-based methods. For sim-
 259 plicity and efficiency, we use the text-matching method by default. More analyses can be found in Appendix C.1.

layer as it encodes richer and more useful semantic information (Skean et al., 2025; Azaria & Mitchell, 2023; Liu et al., 2019). Inspired by the fact that eigenvalues of the covariance matrix can capture the divergence and correlation between different embeddings (Chen et al., 2024a), we calculate the eigenvalues of the cross-covariance for \mathbf{H}_i^k to measure the diversity of intermediate reasoning steps:

$$\Sigma_i^k = \mathbf{H}_i^{k\top} \cdot \mathbf{J}_d \cdot \mathbf{H}_i^k; \quad \text{Eig}_i^k = \frac{1}{m} \log \det(\Sigma_i^k) = \frac{1}{m} \sum_{u=1}^m \log(\lambda_{i,u}^k), \quad (4)$$

where $\mathbf{J}_d = \mathbf{I}_d - \frac{1}{d} \mathbf{1}_{d \times d}$ is the centering matrix, $\mathbf{I}_d \in \mathbb{R}^d$ is the identity matrix, $\mathbf{1}_{d \times d} \in \mathbb{R}^{d \times d}$ is the all-one matrix, $\det(\cdot)$ means the determinant of matrix, and $\{\lambda_{i,u}^k\}_{u=1}^m$ denotes the singular values of matrix Σ_i^k . Furthermore, considering that some important tokens with higher attention weights might contribute more to the reasoning process, we enhance the above method via an attention-aware weighting mechanism. In practice, following the implementation of Su et al. (2024), let $\text{Atten}_{i,u}^k \in (0, 1)$ denote the normalized maximum self-attention weight for u -th token ($u \in [1, m]$) among all self-attention heads, we can obtain our final reasoning diversity metric, denoted as **Intrinsic Diversity** score (*InDiv* in short) to distinguish it from Eq. 3, which is formulated as follows:

$$\text{InDiv}_i^k = \sum_{u=1}^m \left[\text{Atten}_{i,u}^k \cdot \log(\lambda_{i,u}^k) \right]; \quad \sum_{u=1}^m \text{Atten}_{i,u}^k = 1. \quad (5)$$

When the reasoning steps are repetitive and have similar semantics, the hidden representations will be highly correlated, and their semantic entropy and *InDiv* scores will be small (more analyses are in Appendix C.2). After calculating the *InDiv* scores of all candidate correct solutions $\{(x_i, \hat{r}_i^k, \hat{y}_i^k)\}_{k=1}^K$ for x_i , we filter the undesired ones with lower scores. Specifically, inspired by DeepSeek-r1 (Guo et al., 2025), we regularize the scores as $\overline{\text{InDiv}}_i^k = \frac{\text{InDiv}_i^k - \text{mean}(\{\text{InDiv}_i^1, \dots, \text{InDiv}_i^K\})}{\text{std}(\{\text{InDiv}_i^1, \dots, \text{InDiv}_i^K\})}$ and filter the solutions with scores below the threshold τ . Finally, we can obtain more accurate, diverse, and concise reasoning data for effective self-training. The pseudo-code of HSIR is shown in Algorithm 2.

4 EXPERIMENTS

4.1 EXPERIMENTAL SETUP

Tasks and Datasets. We mainly assess the effectiveness of HSIR on both medical reasoning and mathematical reasoning tasks, using the MedQA (Jin et al., 2021) and GSM8K (Cobbe et al., 2021) datasets, respectively. For MedQA, we follow the settings in §2.2, and use 1K reasoning data distilled from DeepSeek-R1 as the seed data \mathcal{S} and the other 8.3K data as the unlabeled dataset \mathcal{D} . Notably, the impact of different seed data can be found in Appendix C.4. For GSM8K, we use the 6.9K reasoning dataset released by CAMEL (Li et al., 2023). Similarly, 1K reasoning samples are randomly selected to form \mathcal{S} , while the remaining samples form \mathcal{D} . More specifically, the reasoning template is similar to that in DeepSeek-R1, i.e., the reasoning process and answer are enclosed with `<think>/<think>` and `<answer>/<answer>` tags. Some training data examples are provided in Table 7 and 8. For evaluation, we report the zero-shot results on the original test sets of MedQA and GSM8K using the average accuracy and number of generated tokens as metrics. Since all models are evaluated on the same hardware, the number of generated tokens can reflect the wall-clock inference latency.

Training Details. We conduct main experiments using Qwen2.5-1.5B/3B/7B instruct models. To verify the generality of HSIR, we also evaluate it on another four instruct LLMs, including Qwen3-1.7B (Yang et al., 2025a), Phi-3.5-mini (Abdin et al., 2024), Mistral-7B (Jiang et al., 2023), and LLaMA3-8B (Dubey et al., 2024). During the implementation of HSIR, the sampling times K and J are set to 10 and 5, respectively. The sampling temperature is 1.0, and the maximum output length is 2,048. The filter threshold τ is set to -0.5. For the post-training of Qwen2.5 models, the self-improvement iteration T is set to 3, but for the other LLMs, it is set to 1 due to limited computational resources. During inference, we use greedy decoding with a temperature of 0 for reproducibility. The maximum output length for all models is set to 4,096. More dataset and training details are shown in Appendix B, and the efficiency analysis of HSIR is shown in Appendix C.7.

Baselines. To verify the superiority of HSIR, we compare it with various training-based baselines:

- **SFT-Initial:** Standard fine-tuning \mathcal{M}_{base} on the seed data \mathcal{S} to obtain the initial SFT model \mathcal{M}_0 .

Table 1: **Performance comparison between Qwen2.5 family models** using different training methods on MedQA and GSM8K. “|Train|” denotes the [average number of training samples](#) among all models and tasks, while “Overall” denotes the average accuracy and number of output tokens.

Methods	Train	Qwen2.5-1.5B		Qwen2.5-3B		Qwen2.5-7B		Overall	
		Avg.	MedQA	GSM8K	MedQA	GSM8K	MedQA	GSM8K	Accuracy
SFT-Initial	1.0K	38.10	63.99	49.02	77.18	62.45	83.93	62.45	1,536
SFT-Oracle	8.1K	46.58	71.57	58.68	84.31	73.99	87.79	70.49 ^{+8.04}	1,392 _{-9.4%}
<i>(a) Iterative Self-improvement SFT Training</i>									
RFT	132.2K	42.42	71.19	54.60	83.55	64.89	87.87	67.42 ^{+4.97}	1292 _{-15.9%}
ReGenesis	127.2K	44.46	66.26	50.67	79.91	62.22	89.99	65.59 ^{+3.13}	363
STaR									
Iteration 1	5.7K	35.98	69.75	49.25	81.96	61.19	87.72	64.31 ^{+1.86}	1,379 _{-10.2%}
Iteration 2	6.1K	37.78	70.96	50.82	81.27	61.04	88.48	65.06 ^{+2.61}	1,328 _{-13.5%}
Iteration 3	6.4K	38.49	72.02	47.76	81.58	61.59	87.49	64.82 ^{+2.37}	1,288 _{-16.1%}
ReST ^{EM}									
Iteration 1	44.7K	41.63	69.75	55.22	83.95	64.18	88.17	67.15 ^{+4.70}	1,268 _{-17.5%}
Iteration 2	51.0K	42.81	74.45	56.25	85.13	65.28	90.22	69.02 ^{+6.57}	1,160 _{-24.5%}
Iteration 3	53.6K	45.48	75.13	56.48	86.04	65.28	89.99	69.73 ^{+7.28}	1,114 _{-27.5%}
HStR-SFT (Ours)									
Iteration 1	33.6K	45.33	71.72	55.70	86.13	67.32	88.78	69.16 ^{+6.71}	1,075 _{-30.0%}
Iteration 2	36.6K	46.50	76.04	56.32	86.51	67.87	90.83	70.68 ^{+8.23}	950 _{-38.1%}
Iteration 3	38.8K	46.58	76.88	57.58	86.81	68.74	91.36	71.33 ^{+8.88}	896 _{-41.7%}
<i>(b) Iterative Self-improvement DPO Training</i>									
IRPO									
Iteration 1	22.7K	39.04	70.51	47.99	85.37	64.26	91.43	66.43 ^{+3.98}	1,359 _{-11.5%}
Iteration 2	27.5K	41.08	75.51	49.33	86.66	63.24	91.95	67.96 ^{+5.51}	1,294 _{-15.7%}
Iteration 3	20.5K	43.91	75.36	49.10	87.19	60.57	91.87	68.00 ^{+5.55}	1,271 _{-17.2%}
HStR-DPO (Ours)									
Iteration 1	17.9K	48.31	75.36	55.77	87.04	67.32	91.36	70.86 ^{+8.41}	1,007 _{-34.4%}
Iteration 2	23.6K	49.10	76.65	59.15	87.49	68.58	91.96	72.16 ^{+9.70}	921 _{-40.0%}
Iteration 3	19.6K	50.90	78.09	60.64	87.53	70.46	92.49	73.35 ^{+10.90}	885 _{-42.4%}

- **SFT-Oracle**: Standard fine-tuning \mathcal{M}_{base} on the combination of \mathcal{S} and \mathcal{D} with ground-truth reasoning trajectories, which can be considered as the upper bound of SFT training.
- **STaR** (Zelikman et al., 2022): Sampling a solution (\hat{r}_i, \hat{y}_i) using greedy decoding for each query $x_i \in \mathcal{D}$, where the correct solutions are used to iteratively fine-tune the models.
- **ReST^{EM}** (Singh et al., 2023): Extending STaR by sampling K solutions $\{(\hat{r}_i^k, \hat{y}_i^k)\}_{k=1}^K$ for each query $x_i \in \mathcal{D}$, where all correct solutions are used for iterative self-improvement SFT training.
- **RFT** (Yuan et al., 2023): Similar to ReST^{EM} but not iterative. To maintain consistent training budgets, we sample $T \times K$ candidate solutions $\{(\hat{r}_i^k, \hat{y}_i^k)\}_{k=1}^{T \times K}$ for each query $x_i \in \mathcal{D}$.
- **ReGenesis** (Peng et al., 2025): Prompting \mathcal{M}_{base} to self-synthesize reasoning paths by converting general reasoning guidelines into task-specific ones, which are used for once self-training. Since it is not designed for long-CoT reasoning, we do not compare its reasoning efficiency.
- **IRPO** (Pang et al., 2024): Sampling K solutions for each query, where both correct and incorrect solutions are paired to construct the preference data, allowing for iterative DPO training.

For all baselines, we keep a fixed data synthesis budget. Moreover, since our goal is to propose a self-improvement training method, we do not compare HSIR with inference-time methods in the main experiments. More comparisons with inference-time methods are shown in Appendix C.9.

4.2 MAIN RESULTS

HSIR outperforms the other baseline methods across all post-training settings. Table 1 reports the comparative results (%) of Qwen2.5 family models. As seen, self-improvement training on the relatively simple GSM8K task performs better against the challenging MedQA task, confirming that self-improvement methods fall short in complex reasoning tasks. More specifically, during SFT on MedQA, STaR struggles to enhance the LRM_s’ reasoning performance, and even leads to performance degradation, *e.g.*, from 38.10% to 35.98% in Qwen2.5-1.5B. By sampling more diverse solutions, RFT and ReST^{EM} alleviate this problem, indicating the importance of self-training with diverse reasoning data. While in the DPO phase, the effectiveness of self-improvement is more

378 Table 2: **Performance comparison between the other models** using different self-improvement SFT
 379 methods on MedQA and GSM8K. Here, we perform the self-improvement training for one iteration.
 380

381 Methods	382 Qwen3-1.7B		383 Phi-3.5-mini		384 Mistral-7B		385 LLaMA3-8B		386 Overall	
	387 MedQA	388 GSM8K	389 MedQA	390 GSM8K	391 MedQA	392 GSM8K	393 MedQA	394 GSM8K	395 Accuracy	396 Tokens
SFT-Initial	51.61	87.03	66.14	82.56	55.93	64.59	64.57	79.98	69.05	1,540
SFT-Oracle	55.77	87.72	74.07	87.95	70.15	79.08	73.76	86.73	76.90 ^{↑7.85}	1,383 ^{↓10.2%}
STaR	52.87	86.96	65.99	86.28	53.57	68.54	59.63	80.59	69.30 ^{↑0.25}	1,442 ^{↓6.3%}
ReST ^{EM}	54.67	88.61	67.64	87.86	58.13	72.71	67.79	81.20	72.33 ^{↑3.28}	1,365 ^{↓11.4%}
HSIR-SFT	55.30	89.16	71.17	88.32	61.27	75.82	69.68	86.66	74.67^{↑5.62}	1,195^{↓22.4%}

387 dependent on the quality of self-generated data, as preference learning is more data-sensitive. By
 388 selecting more diverse and concise self-generated data for training, our HSIR can effectively unleash
 389 the reasoning abilities of LRM_s, thus achieving better performance against the other baselines.
 390 For instance, our HSIR-DPO outperforms the vanilla iterative DPO method by a clear margin, *i.e.*,
 391 bringing +5.35% average performance gains among all Qwen2.5 models after three iterations.
 392

393 **HSIR effectively improves the reasoning performance and efficiency of LRM_s in both tasks.**
 394 In addition to the reasoning performance, we also evaluate the reasoning efficiency of LRM_s by
 395 measuring the number of output tokens. From Table 1, it can be seen that nearly all self-improvement
 396 methods reduce the average output tokens. We conjecture that models can sometimes generate concise
 397 reasoning paths, which helps guide the efficient reasoning of models. Nevertheless, as shown in our
 398 preliminary analysis (§2.2), self-training with overthinking solutions would damage this effect and
 399 lead to suboptimal reasoning efficiency. Owing to our *InDiv* metric, we can filter these overthinking
 400 solutions and effectively improve reasoning efficiency by reducing up to 42.4% output tokens. These
 401 results confirm the significance of alleviating overthinking and prove the effectiveness of HSIR.

402 **HSIR brings consistent and significant performance gains among all model sizes and types.**
 403 Table 2 presents the results of other LRM_s. Notably, due to limited computation resources, we only
 404 perform the SFT training using STaR, ReST^{EM}, and our HSIR for one iteration. As seen, HSIR
 405 continues to outperform the other baseline methods across all models. Specifically, in LLaMA3-8B,
 406 compared to powerful ReST^{EM}, HSIR achieves +1.89% and +5.46% performance gains for MedQA
 407 and GSM8K, respectively. Overall, HSIR brings +5.62% average performance gains and reduces
 408 22.4% output tokens against the initial SFT models, showing its universality and superiority.

409 4.3 MORE ANALYSES

410 **Ablation Study.** In this part, we validate the
 411 important components of HSIR, *i.e.*, *VeriExit*
 412 sampling strategy and *InDiv* metric. Firstly,
 413 for the analysis of sampling strategy, we ignore
 414 the overthinking metric and do not perform the
 415 data filtering. To verify the effectiveness of *VeriExit*,
 416 we compare it with “-w Answer-driven”
 417 that uses the ground-truth answer to guide models’
 418 reasoning for collecting more correct solutions
 419 ([Ding et al., 2025](#)). Similarly, for the analysis
 420 of overthinking metric, we do not use extra
 421 sampling methods, and compare our *InDiv* with
 422 “-w Length-driven” that leverages the length of

423 solutions as the metric. In practice, the candidate solutions with $\frac{\text{len}(\hat{r}_i^k) - \text{mean}(\{\text{len}(\hat{r}_i^1), \dots, \text{len}(\hat{r}_i^K)\})}{\text{std}(\{\text{len}(\hat{r}_i^1), \dots, \text{len}(\hat{r}_i^K)\})} > \tau_{\text{len}}$

424 are filtered, where $\text{len}(\hat{r}_i^k)$ denotes the length of \hat{r}_i^k and τ_{len} is the length threshold set to 0.5 in this
 425 experiment. Table 3 reports the results of Qwen2.5-1.5B models after one iteration of self-improvement
 426 SFT training. Compared to the full HSIR, removing *VeriExit* or *InDiv* results in performance degra-
 427 dation, indicating their effectiveness. Moreover, our proposed methods consistently perform better
 428 than their counterparts. For instance, *VeriExit* outperforms the “-w Answer-driven” by 2.14% average
 429 performance gains. These comparative results demonstrate the superiority of *VeriExit* and *InDiv*.

430 **Expand to GRPO Training.** In addition to SFT and DPO training, reinforcement learning from
 431 verifiable rewards via the GRPO ([Shao et al., 2024](#)) algorithm is also a popular and effective way to

432 Table 3: **Ablation study** on *VeriExit* and *InDiv*.

433 Method	434 MedQA		435 GSM8K	
	436 Accuracy	437 Tokens	438 Accuracy	439 Tokens
SFT-Initial	38.10	1,779	63.99	1,666
STaR	35.98	1,651	69.75	1,377
ReST ^{EM}	41.63	1,424	69.75	1,382
HSIR-SFT (All)	45.33	1,064	71.72	1,181
<i>(a) Analysis of sampling strategy (without data filtering)</i>				
-w/ Answer-driven	41.63	1,421	69.29	1,433
-w/ <i>VeriExit</i> (Ours)	44.46	1,293	70.74	1,361
<i>(b) Analysis of overthinking metric (without extra sampling)</i>				
-w/ Length-driven	42.36	1,321	70.66	1,266
-w/ <i>InDiv</i> (Ours)	42.66	1,260	71.34	1,256

$$\frac{\text{len}(\hat{r}_i^k) - \text{mean}(\{\text{len}(\hat{r}_i^1), \dots, \text{len}(\hat{r}_i^K)\})}{\text{std}(\{\text{len}(\hat{r}_i^1), \dots, \text{len}(\hat{r}_i^K)\})} > \tau_{\text{len}}$$

432 are filtered, where $\text{len}(\hat{r}_i^k)$ denotes the length of \hat{r}_i^k and τ_{len} is the length threshold set to 0.5 in this
 433 experiment. Table 3 reports the results of Qwen2.5-1.5B models after one iteration of self-improvement
 434 SFT training. Compared to the full HSIR, removing *VeriExit* or *InDiv* results in performance degra-
 435 dation, indicating their effectiveness. Moreover, our proposed methods consistently perform better
 436 than their counterparts. For instance, *VeriExit* outperforms the “-w Answer-driven” by 2.14% average
 437 performance gains. These comparative results demonstrate the superiority of *VeriExit* and *InDiv*.

enhance LRM’s reasoning performance. Instead of explicitly supervising the reasoning trajectory, GRPO enables LRM to learn from free exploration via outcome rewards, *e.g.*, binary accuracy reward. Although effective, GRPO training also suffers from the overthinking problem. To this end, we propose to improve the GRPO by leveraging our *InDiv* score as an extra reward, and denote this method as **H-GRPO**. The implementation details of H-GRPO can be found in Appendix A. Intuitively, by encouraging LRM to generate diverse and concise reasoning paths, H-GRPO can effectively alleviate overthinking and result in better performance. It is noteworthy that the calculation of *InDiv* scores is fast and would not lead to much training latency. We apply our H-GRPO to reinforce the M_0 models using the \mathcal{D} dataset, and report the results of Qwen2.5 family models in Table 4.

Table 4: Performance comparison between Qwen2.5 models using different GRPO algorithms.

Methods	Qwen2.5-1.5B		Qwen2.5-3B		Qwen2.5-7B		Overall	
	MedQA	GSM8K	MedQA	GSM8K	MedQA	GSM8K	Accuracy	Tokens
GRPO	46.34	73.08	57.03	82.49	66.46	89.61	69.17	974
+ Long2Short	46.50	72.63	58.21	82.26	66.14	91.13	69.48 ^{±0.31}	668 _{±31.4%}
+ CosFn	47.96	71.72	55.22	82.93	63.71	89.31	68.48 _{±0.69}	966 _{±0.9%}
H-GRPO (Ours)	48.15	74.60	58.98	83.09	68.03	91.43	70.71^{±1.54}	710_{±27.1%}

For comparison, we also employ two widely-used baseline methods: *Long2Short* (Team et al., 2025) and *CosFn* (Yang et al., 2025c), which address overthinking by using length-oriented reward functions. As seen, compared to the vanilla GRPO, all improved methods achieve better reasoning efficiency, indicating the validity of extra rewards. However, both length-oriented methods would cause a decrease in reasoning accuracy, *e.g.*, 1.53% average performance drops in Qwen2.5-7B on MedQA. This indicates that overly emphasizing length reduction might hinder LRM’s deep reasoning and lead to suboptimal results. Conversely, by optimizing the intermediate reasoning process, our H-GRPO can smoothly reduce repetitive and redundant thinking and thus achieve better performance.

Evaluation on more reasoning benchmarks. To verify the generality of our HSIR, we additionally evaluate it on more reasoning tasks. Specifically, we use the AI2 Reasoning Challenge’s challenge set (ARC) (Clark et al., 2018) for scientific reasoning, CommonsenseQA (CSQA) (Talmor et al., 2019) for commonsense reasoning, and StrategyQA (StrQA) (Geva et al., 2021) for multi-hop reasoning. Similar to the settings in §4, DeepSeek-R1 is used to collect the seed data for each task. All data and training details are provided in Appendix B. Table 5 shows the comparative results of Qwen2.5 models. As seen, our HSIR-SFT consistently outperforms the other counterparts by a clear margin. More specifically, compared to the base model, HSIR-SFT brings +5.41% average performance gains and reduces 23.3% average inference tokens. These results can prove the generality of HSIR.

Table 5: Comparison results on more reasoning benchmarks. Notably, we perform the self-improvement SFT training for one iteration in this experiment.

Method	Qwen2.5-1.5B			Qwen2.5-3B			Qwen2.5-7B			Overall	
	ARC	StraQA	CSQA	ARC	StraQA	CSQA	ARC	StraQA	CSQA	Accuracy	Tokens
SFT-Initial	68.33	59.10	60.03	79.91	66.67	71.91	86.43	72.05	73.63	70.90	1298
SFT-Oracle	69.38	60.84	74.20	80.66	69.29	79.69	87.55	74.38	82.47	75.38 ^{±4.48}	1223 _{±5.8%}
STaR	68.58	61.28	62.74	81.20	68.85	73.05	87.98	71.76	74.86	72.26 _{±1.36}	1232 _{±5.1%}
ReST ^{EM}	69.78	62.30	68.14	83.26	68.59	77.64	89.18	72.36	79.19	74.49 ^{±3.59}	1148 _{±11.6%}
HSIR-SFT	72.45	64.63	72.48	83.92	69.59	78.54	89.87	73.65	81.65	76.31^{±5.41}	996_{±23.3%}

Model Generalization. Here, we further investigate the ability of self-improved LRM to generalize to out-of-distribution (OOD) tasks. Specifically, for models trained on MedQA, we evaluate their performance on the Medbullets (4-option) (Chen et al., 2025) and MedXpertQA (Zuo et al., 2025). While for models trained on GSM8K, we evaluate on the MATH (Hendrycks et al., 2021) and AMC2023 (Mathematical Association of America, 2023). We illustrate the OOD results of Qwen2.5-7B models using different self-training methods in Figure 4. From it, we can observe that: (1) Compared to iterative SFT, self-improvement with iterative DPO training can generally result in better OOD performance, similar to the finding of Wu et al. (2025). This is consistent with the wisdom that DPO can improve OOD generalization (Kirk et al., 2024). (2) Both HSIR-SFT and HSIR-DPO can achieve consistently better OOD results against the baseline methods. We attribute it to the *VeriExit* sampling strategy in HSIR as it can collect more diverse solutions for generalized self-training. These results confirm our motivation to mitigate the data imbalance problem.

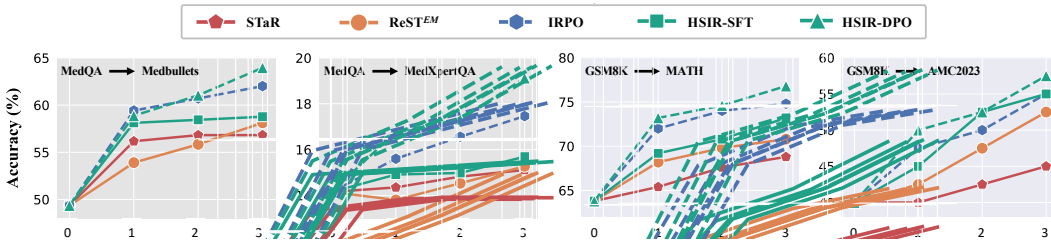


Figure 4: **Comparison of OOD results** between Qwen2.5-7B models trained with different iterative self-improvement methods. The x-axis denotes the index of self-improvement training iteration.

5 RELATED WORK

Recently, post-training the LLMs with explicit reasoning paths via SFT or preference learning algorithms has shown remarkable potential to unleash their reasoning capabilities (Li et al., 2025; Plaat et al., 2024; Wen et al., 2025). However, these methods are highly dependent on extensive, high-quality reasoning trajectories. Notably, although the RLVR paradigm can also enhance models’ reasoning performance without relying on reasoning trajectories (Guo et al., 2025), cold-start training with these trajectories can improve training efficiency and yield higher performance (Yang et al., 2025c). This also underscores the importance of explicit reasoning trajectories. Besides obtaining these trajectories from human experts, a common alternative way is to distill them from a larger proprietary model, which is still costly and time-consuming (Peng et al., 2025).

To address the above issue, recent literature introduces the “self-improvement” paradigm, where models improve themselves using self-generated data without any external supervision (Zelikman et al., 2022; Yuan et al., 2023; Huang et al., 2023; Gulcehre et al., 2023; Wang et al., 2024; Hosseini et al., 2024; Wu et al., 2025; Huang et al., 2025a; Song et al., 2025). However, we reveal that these self-improvement methods usually suffer from data imbalance and overthinking (§2.2). Some prior studies also recognize these problems and attempt to address them by allocating more trials to difficult queries (Tong et al., 2024; Ding et al., 2025; Koh et al., 2025) or designing length-oriented reward functions to penalize too long solutions (Team et al., 2025; Munkhbat et al., 2025). For instance, AdaSTaR (Koh et al., 2025) proposes an adaptive sampling strategy to ensure data balance by prioritizing under-trained examples. While effective, it overlooks the reuse of prior failed solutions and requires a larger inference budget. Moreover, current length-oriented methods may lead to performance degradation due to excessive emphasis on length reduction (Dai et al., 2025).

Different from prior studies, we propose two simple-yet-effective approaches to address these problems efficiently. Specifically, instead of solely allocating more trials to difficult queries, our proposed *VeriExit* strategy attempts to reuse partial correct reasoning steps from previous failed solutions to improve the sampling efficiency. Notably, this technology bears some resemblance to prior early-exit decoding methods (Rahmath P et al., 2024; Yang et al., 2025b), but the idea of reusing previous failed solutions for efficient data synthesis is innovative. To alleviate overthinking, we introduce the *InDiv* score that leverages the internal state of LRM as a signal to encourage models’ diverse and concise reasoning, rather than simply using a length penalty. To the best of our knowledge, our *InDiv* is one of the first works that use the internal states of LRM to guide the concise reasoning during self-improvement training.

6 CONCLUSION

In this paper, we reveal and address the limitations of self-improvement post-training in LRM. Through a series of preliminary analyses, we find that the self-improvement of LRM usually suffers from data imbalance and overthinking in the complex reasoning scenarios. To address these limitations, we propose HSIR, which effectively harnesses self-improvement in LRM via two simple-yet-effective approaches: *VeriExit* sampling strategy and *InDiv* metric. Extensive results show that HSIR consistently and significantly improves the reasoning performance and efficiency across all model sizes and architectures. Moreover, we also expand our method to the RLVR training paradigm and propose H-GRPO that improves the GRPO by leveraging the *InDiv* scores as an extra reward. Comparative results with two widely-used GRPO algorithms prove the superiority of H-GRPO.

540 ETHICS AND REPRODUCIBILITY STATEMENTS
541

542 **Ethics.** We take ethical considerations very seriously and strictly adhere to the ICLR Ethics
543 Policy. This paper proposes a new self-improvement training framework to improve the reasoning
544 performance and efficiency of LRM. It aims to unleash LRM's internal reasoning capabilities,
545 instead of encouraging them to learn privacy knowledge that may cause an ethical problem. Moreover,
546 all base models, training and evaluation datasets used in this paper are publicly available and have
547 been widely adopted by researchers. Thus, we believe that this research will not pose ethical issues.
548

549 **Reproducibility.** In this paper, we discuss the detailed experimental setup, such as training hyper-
550 parameters and statistical descriptions in Appendix B. More importantly, *we have provided our code*
551 *and data in the Supplementary Material* to help reproduce our experimental results.
552

553 REFERENCES
554

555 Marah Abdin, Jyoti Aneja, Hany Awadalla, Ahmed Awadallah, Ammar Ahmad Awan, Nguyen Bach,
556 Amit Bahree, Arash Bakhtiari, Jianmin Bao, Harkirat Behl, et al. Phi-3 technical report: A highly
557 capable language model locally on your phone. *arXiv preprint arXiv:2412.08905*, 2024.

558 Sina Alemohammad, Josue Casco-Rodriguez, Lorenzo Luzi, Ahmed Intiaz Humayun, Hossein
559 Babaei, Daniel LeJeune, Ali Siahkoohi, and Richard Baraniuk. Self-consuming generative models
560 go mad. In *The Twelfth International Conference on Learning Representations*, 2024.

561 Amos Azaria and Tom Mitchell. The internal state of an llm knows when it's lying. In *Findings of*
562 *the Association for Computational Linguistics: EMNLP 2023*, 2023.

563 Quentin Bertrand, Joey Bose, Alexandre Duplessis, Marco Jiralerspong, and Gauthier Gidel. On the
564 stability of iterative retraining of generative models on their own data. In *The Twelfth International*
565 *Conference on Learning Representations*, 2024.

566 Chao Chen, Kai Liu, Ze Chen, Yi Gu, Yue Wu, Mingyuan Tao, Zhihang Fu, and Jieping Ye. Inside:
567 Llms' internal states retain the power of hallucination detection. In *The Twelfth International*
568 *Conference on Learning Representations*, 2024a.

569 Hanjie Chen, Zhouxiang Fang, Yash Singla, and Mark Dredze. Benchmarking large language models
570 on answering and explaining challenging medical questions. In *Proceedings of the 2025 Conference*
571 *of the Nations of the Americas Chapter of the Association for Computational Linguistics: Human*
572 *Language Technologies*, 2025.

573 Jianlyu Chen, Shitao Xiao, Peitian Zhang, Kun Luo, Defu Lian, and Zheng Liu. M3-embedding:
574 Multi-linguality, multi-functionality, multi-granularity text embeddings through self-knowledge
575 distillation. In *Findings of the Association for Computational Linguistics ACL 2024*, 2024b.

576 Junying Chen, Zhenyang Cai, Ke Ji, Xidong Wang, Wanlong Liu, Rongsheng Wang, Jianye Hou,
577 and Benyou Wang. Huatuogpt-01, towards medical complex reasoning with llms. *arXiv preprint*
578 *arXiv:2412.18925*, 2024c.

579 Xingyu Chen, Jiahao Xu, Tian Liang, Zhiwei He, Jianhui Pang, Dian Yu, Linfeng Song, Qizhi Liu,
580 Mengfei Zhou, Zhuosheng Zhang, et al. Do not think that much for $2+3=?$ on the overthinking of
581 o1-like llms. *arXiv preprint arXiv:2412.21187*, 2024d.

582 Zeming Chen, Alejandro Hernández Cano, Angelika Romanou, Antoine Bonnet, Kyle Matoba,
583 Francesco Salvi, Matteo Pagliardini, Simin Fan, Andreas Köpf, Amirkeivan Mohtashami,
584 et al. Meditron-70b: Scaling medical pretraining for large language models. *arXiv preprint*
585 *arXiv:2311.16079*, 2023.

586 Peter Clark, Isaac Cowhey, Oren Etzioni, Tushar Khot, Ashish Sabharwal, Carissa Schoenick, and
587 Oyvind Tafjord. Think you have solved question answering? try arc, the ai2 reasoning challenge.
588 *arXiv preprint arXiv:1803.05457*, 2018.

594 Karl Cobbe, Vineet Kosaraju, Mohammad Bavarian, Mark Chen, Heewoo Jun, Lukasz Kaiser,
 595 Matthias Plappert, Jerry Tworek, Jacob Hilton, Reiichiro Nakano, et al. Training verifiers to solve
 596 math word problems. *arXiv preprint arXiv:2110.14168*, 2021.

597

598 Muzhi Dai, Chenxu Yang, and Qingyi Si. S-grpo: Early exit via reinforcement learning in reasoning
 599 models. *arXiv preprint arXiv:2505.07686*, 2025.

600

601 Yiwen Ding, Zhiheng Xi, Wei He, Lizhuoyuan Lizhuoyuan, Yitao Zhai, Shi Xiaowei, Xunliang Cai,
 602 Tao Gui, Qi Zhang, and Xuan-Jing Huang. Mitigating tail narrowing in llm self-improvement via
 603 socratic-guided sampling. In *Proceedings of the 2025 Conference of the Nations of the Americas*
 604 *Chapter of the Association for Computational Linguistics: Human Language Technologies*, 2025.

605

606 Abhimanyu Dubey, Abhinav Jauhri, Abhinav Pandey, Abhishek Kadian, Ahmad Al-Dahle, Aiesha
 607 Letman, Akhil Mathur, Alan Schelten, Amy Yang, Angela Fan, et al. The llama 3 herd of models.
 608 *arXiv e-prints arXiv: 2407.21783*, 2024.

609

610 Matthias Gerstgrasser, Rylan Schaeffer, Apratim Dey, Rafael Rafailev, Tomasz Korbak, Henry
 611 Sleight, Rajashree Agrawal, John Hughes, Dhruv Bhandarkar Pai, Andrey Gromov, et al. Is model
 612 collapse inevitable? breaking the curse of recursion by accumulating real and synthetic data. In
 613 *First Conference on Language Modeling*, 2024.

614

615 Mor Geva, Daniel Khashabi, Elad Segal, Tushar Khot, Dan Roth, and Jonathan Berant. Did aristotle
 616 use a laptop? a question answering benchmark with implicit reasoning strategies. *Transactions of*
 617 *the Association for Computational Linguistics*, 9:346–361, 2021.

618

619 Luis Gonzalo Sanchez Giraldo, Murali Rao, and Jose C Principe. Measures of entropy from data
 620 using infinitely divisible kernels. *IEEE Transactions on Information Theory*, 2014.

621

622 Caglar Gulcehre, Tom Le Paine, Srivatsan Srinivasan, Ksenia Konyushkova, Lotte Weerts, Abhishek
 623 Sharma, Aditya Siddhant, Alex Ahern, Miaosen Wang, Chenjie Gu, et al. Reinforced self-training
 624 (rest) for language modeling. *arXiv preprint arXiv:2308.08998*, 2023.

625

626 Daya Guo, Dejian Yang, Haowei Zhang, Junxiao Song, Ruoyu Zhang, Runxin Xu, Qihao Zhu,
 627 Shirong Ma, Peiyi Wang, Xiao Bi, et al. Deepseek-r1: Incentivizing reasoning capability in llms
 628 via reinforcement learning. *arXiv preprint arXiv:2501.12948*, 2025.

629

630 Dan Hendrycks, Collin Burns, Saurav Kadavath, Akul Arora, Steven Basart, Eric Tang, Dawn
 631 Song, and Jacob Steinhardt. Measuring mathematical problem solving with the math dataset. In
 632 *Thirty-fifth Conference on Neural Information Processing Systems Datasets and Benchmarks Track*
 633 *(Round 2)*, 2021.

634

635 Roger A Horn and Charles R Johnson. *Matrix analysis*. Cambridge university press, 2012.

636

637 Arian Hosseini, Xingdi Yuan, Nikolay Malkin, Aaron Courville, Alessandro Sordoni, and Rishabh
 638 Agarwal. V-star: Training verifiers for self-taught reasoners. In *First Conference on Language*
 639 *Modeling*, 2024.

640

641 Audrey Huang, Adam Block, Dylan J Foster, Dhruv Rohatgi, Cyril Zhang, Max Simchowitz, Jor-
 642 dan T Ash, and Akshay Krishnamurthy. Self-improvement in language models: The sharpening
 643 mechanism. In *The Thirteenth International Conference on Learning Representations*, 2025a.

644

645 Jiaxin Huang, Shixiang Gu, Le Hou, Yuexin Wu, Xuezhi Wang, Hongkun Yu, and Jiawei Han. Large
 646 language models can self-improve. In *Proceedings of the 2023 Conference on Empirical Methods*
 647 *in Natural Language Processing*, 2023.

648

649 Zhongzhen Huang, Gui Geng, Shengyi Hua, Zhen Huang, Haoyang Zou, Shaoting Zhang, Pengfei
 650 Liu, and Xiaofan Zhang. O1 replication journey—part 3: Inference-time scaling for medical
 651 reasoning. *arXiv preprint arXiv:2501.06458*, 2025b.

652

653 Albert Q Jiang, Alexandre Sablayrolles, Arthur Mensch, Chris Bamford, Devendra Singh Chaplot,
 654 Diego de las Casas, Florian Bressand, Gianna Lengyel, Guillaume Lample, Lucile Saulnier, et al.
 655 Mistral 7b. *arXiv preprint arXiv:2310.06825*, 2023.

648 Di Jin, Eileen Pan, Nassim Oufattolle, Wei-Hung Weng, Hanyi Fang, and Peter Szolovits. What
 649 disease does this patient have? a large-scale open domain question answering dataset from medical
 650 exams. *Applied Sciences*, 2021.

651

652 Robert Kirk, Ishita Mediratta, Christoforos Nalmpantis, Jelena Luketina, Eric Hambro, Edward
 653 Grefenstette, and Roberta Raileanu. Understanding the effects of rlhf on llm generalisation and
 654 diversity. In *The Twelfth International Conference on Learning Representations*, 2024.

655

656 Woosung Koh, Wonbeen Oh, Jaein Jang, MinHyung Lee, Hyeongjin Kim, Ah Yeon Kim, Joonkee
 657 Kim, Junghyun Lee, Taehyeon Kim, and Se-Young Yun. Adastar: Adaptive data sampling for
 658 training self-taught reasoners. In *Thirty-Ninth Conference on Neural Information Processing
 Systems*, 2025.

659

660 Guohao Li, Hasan Abed Al Kader Hammoud, Hani Itani, Dmitrii Khizbulin, and Bernard Ghanem.
 661 Camel: Communicative agents for "mind" exploration of large language model society. In *Thirty-
 662 seventh Conference on Neural Information Processing Systems*, 2023.

663

664 Zhong-Zhi Li, Duzhen Zhang, Ming-Liang Zhang, Jiaxin Zhang, Zengyan Liu, Yuxuan Yao, Haotian
 665 Xu, Junhao Zheng, Pei-Jie Wang, Xiuyi Chen, et al. From system 1 to system 2: A survey of
 reasoning large language models. *arXiv preprint arXiv:2502.17419*, 2025.

666

667 Nelson F Liu, Matt Gardner, Yonatan Belinkov, Matthew E Peters, and Noah A Smith. Linguistic
 668 knowledge and transferability of contextual representations. In *Proceedings of the 2019 Conference
 669 of the North American Chapter of the Association for Computational Linguistics: Human Language
 Technologies*, 2019.

670

671 Wei Liu, Weihao Zeng, Keqing He, Yong Jiang, and Junxian He. What makes good data for
 672 alignment? a comprehensive study of automatic data selection in instruction tuning. In *The Twelfth
 673 International Conference on Learning Representations*, 2024.

674

675 Potsawee Manakul, Adian Liusie, and Mark Gales. Selfcheckgpt: Zero-resource black-box hallucina-
 676 tion detection for generative large language models. In *Proceedings of the 2023 conference on
 677 empirical methods in natural language processing*, pp. 9004–9017, 2023.

678

679 Mathematical Association of America. American mathematics competitions, 2023. URL <https://maa-amc.org/amc/amc-competitions/>.

680

681 Seyed Iman Mirzadeh, Mehrdad Farajtabar, Ang Li, Nir Levine, Akihiro Matsukawa, and Hassan
 682 Ghasemzadeh. Improved knowledge distillation via teacher assistant. In *Proceedings of the AAAI
 conference on artificial intelligence*, 2020.

683

684 Tergel Munkhbat, Namgyu Ho, Seo Hyun Kim, Yongjin Yang, Yujin Kim, and Se-Young Yun.
 685 Self-training elicits concise reasoning in large language models. In *Findings of the Association for
 686 Computational Linguistics: ACL 2025*, 2025.

687

688 Richard Yuanzhe Pang, Weizhe Yuan, He He, Kyunghyun Cho, Sainbayar Sukhbaatar, and Jason
 689 Weston. Iterative reasoning preference optimization. In *Advances in Neural Information Processing
 Systems*, 2024.

690

691 Xiangyu Peng, Congying Xia, Xinyi Yang, Caiming Xiong, Chien-Sheng Wu, and Chen Xing.
 692 Regenesis: Llms can grow into reasoning generalists via self-improvement. In *The Thirteenth
 693 International Conference on Learning Representations*, 2025.

694

695 Aske Plaat, Annie Wong, Suzan Verberne, Joost Broekens, Niki van Stein, and Thomas Bäck.
 Reasoning with large language models, a survey. *arXiv e-prints arXiv:2407.11511*, 2024.

696

697 Rafael Rafailov, Archit Sharma, Eric Mitchell, Christopher D Manning, Stefano Ermon, and Chelsea
 698 Finn. Direct preference optimization: Your language model is secretly a reward model. In *Advances
 699 in neural information processing systems*, 2023.

700

701 Haseena Rahmath P, Vishal Srivastava, Kuldeep Chaurasia, Roberto G Pacheco, and Rodrigo S Couto.
 Early-exit deep neural network-a comprehensive survey. *ACM Computing Surveys*, 57(3):1–37,
 2024.

702 Zhihong Shao, Peiyi Wang, Qihao Zhu, Runxin Xu, Junxiao Song, Xiao Bi, Haowei Zhang,
 703 Mingchuan Zhang, YK Li, Yang Wu, et al. Deepseekmath: Pushing the limits of mathemat-
 704 ical reasoning in open language models. *arXiv preprint arXiv:2402.03300*, 2024.

705 Avi Singh, John D Co-Reyes, Rishabh Agarwal, Ankesh Anand, Piyush Patil, Xavier Garcia, Peter J
 706 Liu, James Harrison, Jaehoon Lee, Kelvin Xu, et al. Beyond human data: Scaling self-training for
 707 problem-solving with language models. *Transactions on Machine Learning Research*, 2023.

708 Oscar Skean, Jhoan Keider Hoyos Osorio, Austin J Brockmeier, and Luis Gonzalo Sanchez Giraldo.
 709 Dime: Maximizing mutual information by a difference of matrix-based entropies. *arXiv preprint*
 710 *arXiv:2301.08164*, 2023.

711 Oscar Skean, Md Rifat Arefin, Dan Zhao, Niket Nikul Patel, Jalal Naghiyev, Yann LeCun, and
 712 Ravid Shwartz-Ziv. Layer by layer: Uncovering hidden representations in language models. In
 713 *Forty-second International Conference on Machine Learning*, 2025.

714 Yuda Song, Hanlin Zhang, Carson Eisenach, Sham M Kakade, Dean Foster, and Udaya Ghai. Mind
 715 the gap: Examining the self-improvement capabilities of large language models. In *The Thirteenth*
 716 *International Conference on Learning Representations*, 2025.

717 Weihang Su, Yichen Tang, Qingyao Ai, Zhijing Wu, and Yiqun Liu. Dragin: Dynamic retrieval
 718 augmented generation based on the real-time information needs of large language models. In *Proceedings of the 62nd Annual Meeting of the Association for Computational Linguistics*, 2024.

719 Alon Talmor, Jonathan Herzig, Nicholas Lourie, and Jonathan Berant. Commonsenseqa: A question
 720 answering challenge targeting commonsense knowledge. In *Proceedings of the 2019 Conference of*
 721 *the North American Chapter of the Association for Computational Linguistics: Human Language*
 722 *Technologies, Volume 1 (Long and Short Papers)*, pp. 4149–4158, 2019.

723 Kimi Team, Angang Du, Bofei Gao, Bowei Xing, Changjiu Jiang, Cheng Chen, Cheng Li, Chenjun
 724 Xiao, Chenzhuang Du, Chonghua Liao, et al. Kimi k1. 5: Scaling reinforcement learning with
 725 llms. *arXiv preprint arXiv:2501.12599*, 2025.

726 Yuxuan Tong, Xiwen Zhang, Rui Wang, Ruidong Wu, and Junxian He. Dart-math: Difficulty-aware
 727 rejection tuning for mathematical problem-solving. In *Advances in Neural Information Processing*
 728 *Systems*, 2024.

729 Tianduo Wang, Shichen Li, and Wei Lu. Self-training with direct preference optimization improves
 730 chain-of-thought reasoning. In *Proceedings of the 62nd Annual Meeting of the Association for*
 731 *Computational Linguistics*, 2024.

732 Xuezhi Wang, Jason Wei, Dale Schuurmans, Quoc V Le, Ed H Chi, Sharan Narang, Aakanksha
 733 Chowdhery, and Denny Zhou. Self-consistency improves chain of thought reasoning in language
 734 models. In *International Conference on Learning Representations*, 2023.

735 Liang Wen, Yunke Cai, Fenrui Xiao, Xin He, Qi An, Zhenyu Duan, Yimin Du, Junchen Liu, Tanglifu
 736 Tanglifu, Xiaowei Lv, Haosheng Zou, Yongchao Deng, Shousheng Jia, and Xiangzheng Zhang.
 737 Light-r1: Curriculum SFT, DPO and RL for long COT from scratch and beyond. In *Proceedings*
 738 *of the 63rd Annual Meeting of the Association for Computational Linguistics*, 2025.

739 Ting Wu, Xuefeng Li, and Pengfei Liu. Progress or regress? self-improvement reversal in post-
 740 training. In *The Thirteenth International Conference on Learning Representations*, 2025.

741 Fengli Xu, Qianyue Hao, Zefang Zong, Jingwei Wang, Yunke Zhang, Jingyi Wang, Xiaochong Lan,
 742 Jiahui Gong, Tianjian Ouyang, Fanjin Meng, et al. Towards large reasoning models: A survey of
 743 reinforced reasoning with large language models. *arXiv preprint arXiv:2501.09686*, 2025.

744 An Yang, Baosong Yang, Beichen Zhang, Binyuan Hui, Bo Zheng, Bowen Yu, Chengyuan Li,
 745 Dayiheng Liu, Fei Huang, Haoran Wei, et al. Qwen2. 5 technical report. *arXiv preprint*
 746 *arXiv:2412.15115*, 2024.

747 An Yang, Anfeng Li, Baosong Yang, Beichen Zhang, Binyuan Hui, Bo Zheng, Bowen Yu, Chang
 748 Gao, Chengan Huang, Chenxu Lv, et al. Qwen3 technical report. *arXiv preprint arXiv:2505.09388*,
 749 2025a.

756 Chenxu Yang, Qingyi Si, Yongjie Duan, Zheliang Zhu, Chenyu Zhu, Qiaowei Li, Zheng Lin, Li Cao,
757 and Weiping Wang. Dynamic early exit in reasoning models. *arXiv preprint arXiv:2504.15895*,
758 2025b.

759 Shiming Yang, Yuxuan Tong, Xinyao Niu, Graham Neubig, and Xiang Yue. Demystifying long
760 chain-of-thought reasoning. In *Forty-second International Conference on Machine Learning*,
761 2025c.

762 Qiying Yu, Zheng Zhang, Ruofei Zhu, Yufeng Yuan, Xiaochen Zuo, Yu Yue, Weinan Dai, Tiantian
763 Fan, Gaohong Liu, Lingjun Liu, et al. Dapo: An open-source llm reinforcement learning system at
764 scale. *arXiv preprint arXiv:2503.14476*, 2025.

765 Zheng Yuan, Hongyi Yuan, Chengpeng Li, Guanting Dong, Keming Lu, Chuanqi Tan, Chang Zhou,
766 and Jingren Zhou. Scaling relationship on learning mathematical reasoning with large language
767 models. *arXiv e-prints arXiv: 2308.01825*, 2023.

768 Eric Zelikman, Yuhuai Wu, Jesse Mu, and Noah Goodman. Star: Bootstrapping reasoning with
769 reasoning. In *Advances in Neural Information Processing Systems*, 2022.

770 Chen Zhang, Yang Yang, Jiahao Liu, Jingang Wang, Yunsen Xian, Benyou Wang, and Dawei Song.
771 Lifting the curse of capacity gap in distilling language models. In *Proceedings of the 61st Annual
772 Meeting of the Association for Computational Linguistics*, 2023.

773 Yuxin Zuo, Shang Qu, Yifei Li, Zhang-Ren Chen, Xuekai Zhu, Ermo Hua, Kaiyan Zhang, Ning Ding,
774 and Bowen Zhou. Medxpertqa: Benchmarking expert-level medical reasoning and understanding.
775 In *Forty-second International Conference on Machine Learning*, 2025.

776

777

778

779

780

781

782

783

784

785

786

787

788

789

790

791

792

793

794

795

796

797

798

799

800

801

802

803

804

805

806

807

808

809

Algorithm 1 Reasoning Diversity Metric

```

810
811 1: Input: self-generated reasoning trajectory  $\hat{r}_i^k = [\hat{r}_{i,1}^k, \dots, \hat{r}_{i,L}^k]$ , similarity threshold  $\tau_{\text{sim}}$ 
812 2: Output: reasoning diversity score  $\rho_i^k$ 
813 3: Initialize Empty Unfiltered Set  $\mathcal{U}$ 
814 4: for Each reasoning step  $\hat{r}_{i,l}^k \in \hat{r}_i^k$  do
815 5:   Obtaining the sentence embedding  $\text{emb}(\hat{r}_{i,l}^k)$  using the BGE-m3 model
816 6:   //  $\text{Cos}(\text{emb}(\hat{r}_{i,l}^k), \mathcal{U})$  denotes the cosine distance between  $\text{emb}(\hat{r}_{i,l}^k)$  and its nearest neighbor in  $\mathcal{U}$ 
817 7:   if  $\text{Cos}(\text{emb}(\hat{r}_{i,l}^k), \mathcal{U}) < \tau_{\text{sim}}$  then
818 8:      $\mathcal{U} \leftarrow \mathcal{U} \cup \hat{r}_{i,l}^k$ 
819 9:   else
820 10:    Continue
821 11:   end if
822 12: end for
823 13: Return:  $\rho_i^k = \frac{|\mathcal{U}|}{|[\hat{r}_{i,1}^k, \dots, \hat{r}_{i,L}^k]|}$ 
824
825
826
827

```

A IMPLEMENTATION OF H-GRPO

Background of GRPO and RLVR. Group Relative Policy Optimization (GRPO) (Shao et al., 2024) is a popular RL algorithm, which is widely used in the current popular RLVR training paradigm. Formally, let $\mathcal{M}_{\theta_{\text{ref}}}$ and $\mathcal{M}_{\theta_{\text{new}}}$ denote the reference model and current policy model, GRPO samples a group of solutions $\{(\hat{r}_i^g, \tilde{y}_i^g)\}_{g=1}^G$ for each query $x_i \in \mathcal{D}$, where G denotes the number of solutions in a group. For ease of description, we simplify the solution $(\hat{r}_i^g, \tilde{y}_i^g)$ as a_i^g . Then, we can optimize the $\mathcal{M}_{\theta_{\text{new}}}$ by maximizing the GRPO objective. Notably, inspired by Yu et al. (2025) who use a token-level policy gradient loss to address the unhealthy increase in response length problem of the vanilla GRPO method, we employ an improved token-level GRPO objective function as:

$$\mathcal{J}_{\text{GRPO}}(\theta) = \mathbb{E}[x_i \in \mathcal{D}, \{a_i^g\}_{g=1}^G \sim \mathcal{M}_{\theta_{\text{ref}}}(\cdot | x_i)] \frac{1}{\sum_{g=1}^G |a_i^g|} \sum_{g=1}^G \sum_{o=1}^{|a_i^g|} \left(\min(z_o(a_i^g | x_i) A_g, \text{clip}(z_o(a_i^g | x_i), 1 - \epsilon, 1 + \epsilon) A_g) - \gamma \mathbb{D}_{KL}(\mathcal{M}_{\theta_{\text{new}}} || \mathcal{M}_{\theta_{\text{ref}}}) \right), \quad (6)$$

$$z_o(a_i^g | x_i) = \frac{\mathcal{M}_{\theta_{\text{new}}}(a_{i,o}^g | x_i, a_{i,<o}^g)}{\mathcal{M}_{\theta_{\text{ref}}}(a_{i,o}^g | x_i, a_{i,<o}^g)}, \quad (7)$$

where ϵ and γ are hyper-parameters set to 0.2 and 0.04, respectively, \mathbb{D}_{KL} is a KL penalty term, and A_g is the advantage computed as follows:

$$A_g = \frac{R_g - \text{mean}(\{R_1, R_2, \dots, R_G\})}{\text{std}(\{R_1, R_2, \dots, R_G\})}, \quad (8)$$

where R_g denotes the outcome reward of g -th ($g \in [1, G]$) solution in the group. In the reasoning tasks that contain clear and verifiable answers, e.g., mathematical reasoning, the reward R_g mainly consists of two types of rewards:

- **Accuracy reward** R^{accuracy} : It evaluates whether the solution is correct, i.e., $\mathbb{I}(\tilde{y}_i^g, y_i) = 1$.
- **Format reward** R^{format} : It evaluates whether the defined tags are present in the final solution, i.e., ‘<think>’ and ‘</think>’, ‘<answer>’ and ‘</answer>’ tags.

Reward of H-GRPO. To alleviate the overthinking problem in the vanilla GRPO, we propose H-GRPO, which improves the GRPO by leveraging our *InDiv* scores as an extra reward. Specifically, for each solution in a group, we calculate its *InDiv* score as Eq. 5, and further normalize the score as:

$$R_g^{\text{InDiv}} = \frac{\text{InDiv}^g}{\max(\{\text{InDiv}^1, \dots, \text{InDiv}^G\})}, \quad (9)$$

where $\max(\cdot)$ denotes the maximum *InDiv* scores in a group. The final reward for H-GRPO is the combination of all rewards:

$$R_g^{\text{all}} = R_g^{\text{accuracy}} + R_g^{\text{format}} + \omega \cdot R_g^{\text{InDiv}}, \quad (10)$$

where ω is a coefficient to control the weight of R_g^{InDiv} , which is set to 0.2 in our experiments.

864 **Algorithm 2** Self-improvement Training with HSIR

865

866 1: **Input:** base model \mathcal{M}_{base} , seed data $\mathcal{S} = \{(x_i, r_i, y_i)\}_{i=1}^N$, unlabeled dataset $\mathcal{D} = \{(x_i, y_i)\}_{i=1}^M$

867 2: **Output:** self-improved model \mathcal{M}_T

868 3: Fine-tune \mathcal{M}_{base} on \mathcal{S} to get initial reasoning model \mathcal{M}_0

869 4: **for** $t \in [1, T]$ **do**

870 5: **# Self-generation**

871 6: Obtain K solutions $\{(\hat{r}_i^k, \hat{y}_i^k)\}_{k=1}^K$ generated by \mathcal{M}_{t-1} for each $x_i \in \mathcal{D}$

872 7: Verify the correctness of self-generated solutions, and split them into two groups:

873 $\hat{\mathcal{D}}_t^{correct} = \{(x_i, \hat{r}_i^k, \hat{y}_i^k) \mid x_i \in \mathcal{D}; k \in [1, K]; \mathbb{I}(\hat{y}_i^k, y_i) = 1\}$

874 $\hat{\mathcal{D}}_t^{wrong} = \{(x_i, \hat{r}_i^k, \hat{y}_i^k) \mid x_i \in \mathcal{D}; k \in [1, K]; \mathbb{I}(\hat{y}_i^k, y_i) = 0\}$

875 8:

876 9: **# VeriExit sampling process**

877 10: **for** Each sample $(x_i, \hat{r}_i^k, \hat{y}_i^k) \in \hat{\mathcal{D}}_t^{wrong}$ **do**

878 11: **for** Each reasoning step $\hat{r}_{i,l}^k \in [\hat{r}_{i,1}^k, \dots, \hat{r}_{i,L}^k]$ **do**

879 12: **if** $\hat{r}_{i,l}^k$ arrives at y_i **then**

880 13: Obtain a new query “ $x_i + [\hat{r}_{i,1}^k, \dots, \hat{r}_{i,l}^k] + \text{\textbackslash n\textbackslash n\textltthink\textgt\textbackslash n\textltanswer\textgt\textbackslash n}$ ”

881 14: Feed the new query into \mathcal{M}_{t-1} to resample J answers $\{\hat{y}_i^{k,j}\}_{j=1}^J$

882 15: **Break**

883 16: **else**

884 17: **Continue**

885 18: **end if**

886 19: **end for**

887 20: **end for**

888 21: Build a new dataset $\hat{\mathcal{D}}_t^{VeriExit} = \{(x_i, \hat{r}_{i,1}^k, \dots, \hat{r}_{i,L}^k, \hat{y}_i^{k,j}) \mid \mathbb{I}(\hat{y}_i^{k,j}, y_i) = 1; k \in [1, K]; j \in [1, J]\}$

889 22: Merge $\hat{\mathcal{D}}_t^{VeriExit}$ into $\hat{\mathcal{D}}_t^{correct}$ to obtain the dataset with all correct solutions

890 23:

891 24: **# Calculate the InDiv score**

892 25: **for** Each query $x_i \in \hat{\mathcal{D}}_t^{correct}$ **do**

893 26: Calculate the InDiv score InDiv_i^k for each correct solution $(\hat{r}_i^k, \hat{y}_i^k)_{k=1}^K$ as Eq. 5

894 27: Get the regularized InDiv score $\overline{\text{InDiv}}_i^k = \frac{\text{InDiv}_i^k - \text{mean}(\{\text{InDiv}_i^1, \dots, \text{InDiv}_i^K\})}{\text{std}(\{\text{InDiv}_i^1, \dots, \text{InDiv}_i^K\})}$ for k -th solution

895 28: Update the dataset $\hat{\mathcal{D}}_t^{correct}$ by filtering the undesired solution with $\overline{\text{InDiv}}_i^k < \tau$

896 29: **end for**

897 30:

898 31: **# SFT Training**

899 32: Fine-tune \mathcal{M}_{base} with \mathcal{L}_{SFT} in Eq. 1 on the combination of \mathcal{S} and $\hat{\mathcal{D}}_t^{correct}$

900 33: **# or DPO Training**

901 34: Obtain a pairwise dataset $\hat{\mathcal{D}}_t^{\text{pairs}} = \{(x_i, \hat{r}_i^{k_w}, \hat{y}_i^{k_w}), (x_i, \hat{r}_i^{k_l}, \hat{y}_i^{k_l}) \mid x_i \in \hat{\mathcal{D}}_t; k_w, k_l \in [1, K]\}$,
 where $(\hat{r}_i^{k_w}, \hat{y}_i^{k_w}) \sim \hat{\mathcal{D}}_t^{correct}$ and $(\hat{r}_i^{k_l}, \hat{y}_i^{k_l}) \sim \hat{\mathcal{D}}_t^{wrong}$

902 35: Continually train \mathcal{M}_{t-1} with $\mathcal{L}_{DPO+NLL}$ in Eq. 2 on $\hat{\mathcal{D}}_t^{\text{pairs}}$

903 36: **end for**

904 **More analyses of Table 4.** We present the results of Qwen2.5 models trained with different GRPO
 905 methods in Table 4. Some readers may wonder why the output length of the tuned model significantly
 906 decreases after GRPO training, compared to the initial SFT, *i.e.*, from 1,540 to 987 average tokens.
 907 We conjecture that there are two main reasons. On the one hand, the token-level loss function used in
 908 the improved GRPO algorithm (Eq. 6) can effectively alleviate the abnormal increase in response
 909 length (Yu et al., 2025). On the other hand, according to the public experimental record² of ms-swift³,
 910 during the GRPO training, the solution length initially decreases and then increases, indicating that
 911 the model changed its reasoning manner. Since the GRPO training is computationally expensive,
 912 we do not train the models for very long steps. That is, the training of our models may still be in
 913 the stage of decreasing output length. Despite all this, our H-GRPO can further reduce the inference
 914 overhead, while achieving better reasoning performance. These results can prove the superiority of
 915 H-GRPO, and we believe that it has great potential to perform better after longer GRPO training.
 916 Notably, the aim of this experiment is not to propose a new state-of-the-art GRPO method, but

²<https://swift.readthedocs.io/en/latest/BestPractices/GRPO.html#grpo-training-experiment-record>

³<https://github.com/modelscope/ms-swift>

918 rather to examine whether our proposed *InDiv* method can be incorporated into GRPO to effectively
 919 mitigate the over-thinking problem and address the performance degradation induced by existing
 920 length-oriented rewards. Therefore, we only compare our H-GRPO with two representative GRPO
 921 algorithms that rely on length-oriented rewards. In future work, we plan to further investigate how
 922 *VeriExit* and *InDiv* can be jointly incorporated into GRPO to achieve greater improvements in both
 923 training efficiency and reasoning performance.

925 B MORE EXPERIMENTAL DETAILS

927 B.1 DATASET DETAILS

929 In this work, we evaluate the trained models on several representative and challenging reasoning
 930 benchmarks. Here, we introduce the descriptions of these tasks. Specifically,

- 931 • **MedQA**: MedQA (Jin et al., 2021) is a challenging medical question-answering task, which
 932 consists of questions and corresponding 4-option or 5-option answers in the style of the US
 933 Medical License Exam (USMLE). Since the original MedQA training set does not contain the
 934 reasoning trajectories, we prompt the DeepSeek-R1 to generate the reasoning data. The prompt is
 935 shown in Table 6, and Table 7 presents a case of distilled reasoning trajectories. For in-distribution
 936 evaluation, we follow prior works (Chen et al., 2023) and use the 4-option MedQA with 1,273
 937 samples as the test set.
- 938 • **GSM8K**: GSM8K (Cobbe et al., 2021) is a widely-used mathematical reasoning task, which
 939 contains 8.5K high-quality grade school math word problems. Since the original GSM8K does
 940 not contain any reasoning trajectories, we alternatively use the GSM8K version⁴ released by
 941 CAMEL (Li et al., 2023). Notably, the dataset is also distilled from the DeepSeek-R1. Table 8
 942 presents a case of distilled GSM8K training data. For in-distribution evaluation, we directly use
 943 the original GSM8K with 1.32K test samples.
- 944 • **Medbullets**: Medbullets (Chen et al., 2025) comprises 308 difficult USMLE Step 2&3 style
 945 medical questions collected from real-world conversations. Each question is paired with a case
 946 description and multiple answer choices. In our work, we use the 4-option Medbullets as the OOD
 947 test set of LRMAs trained on MedQA.
- 948 • **MATH**: MATH (Hendrycks et al., 2021) comprises 500 problems spanning five core mathematical
 949 domains: algebra, combinatorics, geometry, number theory, and precalculus. Each problem is
 950 designed to test the multi-step and complex reasoning abilities of LRMAs, requiring more than
 951 simple calculation or knowledge recall. In our experiments, we use this challenging dataset to
 952 evaluate the OOD performance of models trained on GSM8K.
- 953 • **MedXpertQA**: MedXpertQA (Zuo et al., 2025) contains 4,460 high-difficulty medical questions
 954 spanning 17 specialties and 11 body systems. It includes two subsets, MedXpertQA Text for
 955 text medical evaluation and MedXpertQA MM for multimodal medical evaluation. We use the
 956 MedXpertQA Text as the OOD test set of LRMAs trained on MedQA.
- 957 • **AMC2023**: AMC2023 (Mathematical Association of America, 2023) consists of 40 challenging
 958 mathematical problems from American Mathematics Competitions, which is widely used to
 959 evaluate the complex reasoning performance of LRMAs. We use the public test set⁵ to evaluate the
 960 OOD performance of models trained on GSM8K.
- 961 • **ARC**: AI2 Reasoning Challenge’s challenge set (ARC) (Clark et al., 2018) is a scientific reasoning
 962 dataset that contains 1.12K multiple-choice science QA training samples and 1.17K test samples.
 963 Similar to MedQA, we prompt the DeepSeek-R1 to generate the reasoning steps for the training
 964 samples, and randomly select 500 samples as the seed data, using the remaining training samples
 965 as unlabeled data. The trained models are evaluated on the ARC test set.
- 966 • **CommonsenseQA**: CommonsenseQA (CSQA) (Talmor et al., 2019) is a multiple-choice question-
 967 answering dataset that requires diverse types of commonsense knowledge to predict the correct
 968 answers. It contains 12,102 questions, each with one correct answer and four distractors. Similarly,
 969 For the 9.74K training samples, we distill reasoning steps from DeepSeek-R1 and randomly select
 970 1K samples as seed data. The trained models are evaluated on the 1.14K test samples.

⁴https://huggingface.co/datasets/camel-ai/gsm8k_distilled

⁵<https://huggingface.co/datasets/zwhe99/amc23>

972 • **StrategyQA:** StrategyQA (StraQA) (Geva et al., 2021) is an implicit multi-hop reasoning bench-
 973 mark, which contains 1.6K training samples and 687 test samples. After distilling the reasoning
 974 steps from DeepSeek-R1 for the training samples, we randomly select 500 training samples as the
 975 seed data. The trained models are directly evaluated on the test samples.

976

977 B.2 TRAINING AND EVALUATION DETAILS

978

979 In the SFT phase, we fine-tune each model with a batch size of 8 and a peak learning rate of 1e-5,
 980 except 2e-6 for 7B/8B models. In the DPO phase, the batch size is set to 16, and the peak learning rates
 981 for smaller (1.5B/3B) models and larger(7B/8B) models are set to 1e-6 and 2e-7, respectively. In both
 982 training settings, the warm-up ratio is 0.1, and the maximum tokenizer length is 2,048. All models
 983 are trained with full parameter fine-tuning for 3 epochs. We use the popular `LLaMA-Factory`⁶ as
 984 the training codebase.

985 For the RLVR training, we implement the GRPO with the `open-r1`⁷ framework. The rollout size for
 986 each query is set to 8, the learning rate is set to 1e-6, and the batch size is set to 14. Since the GRPO
 987 training is time-consuming and costly, we only train the models for 300 steps. For the implementation
 988 of our H-GRPO, the coefficient ω to control the weight of R^{InDiv} is set to 0.2. All experiments are
 989 conducted on 8 NVIDIA A800 (80GB) GPUs.

990 During evaluation, we sample the model responses by using the greedy decoding method, *i.e.*,
 991 temperature set to 0 for reproducibility. The maximum output length is set 4,096. All models are
 992 evaluated in a zero-shot manner. We extract the final answer from the model response according to
 993 the given format. If no valid answer is extracted, the response is considered incorrect.

994

995 **Table 6: Prompts used for distilling reasoning paths** for MedQA from DeepSeek-R1.

996

997 **System Prompt:**

998 You are a helpful medical AI Assistant. Your task is to select one correct answer from
 999 A to D for the medical question. Please respond in the following format: ‘##Explanation:
 1000 [explanation]\n\n##Answer:\n[option]’

1001

1002 **User Prompt:**

1003 For the following medical question, select one correct answer from A to D.

1004 *Question:* {Question}

1005 *Options:*

1006 A. {Option-A}
 1007 B. {Option-B}
 1008 C. {Option-C}
 1009 D. {Option-D}

1010

1011 **Table 7: An example of seed data in MedQA** distilled from DeepSeek-R1.

1012

1013 **System Prompt:**

1014 You are a helpful medical AI Assistant that provides well-reasoned and detailed responses for
 1015 medical questions. You first think about the reasoning process as an internal monologue and
 1016 then provide the user with the concise and accurate answer. Respond in the following format:
 1017 <think>\n...\n</think>\n<answer>\n...\n</answer>

1018

1019 **Instruction:**

1020 For the following medical question, select one correct answer from A to D.

1021

1022

1023

1024

1025 ⁶<https://github.com/hiyouga/LLaMA-Factory>

⁷<https://github.com/huggingface/open-r1>

1026
 1027 *Question:* A 55-year-old woman comes to the physician because of fevers for 2 weeks. She
 1028 works as a nurse and recently returned from a charity work trip to India, where she worked in a
 1029 medically-underserved rural community. A tuberculin skin test 3 months ago prior to her trip
 1030 showed an induration of 3 mm. Physical examination is unremarkable. An x-ray of the chest
 1031 shows right-sided hilar lymphadenopathy. A sputum culture shows acid-fast bacilli. Which of the
 1032 following immunologic processes most likely occurred first?

1033 *Options:*

1034 A. Formation of a nodular tubercle in the lung
 1035 B. Replication of bacteria within alveolar macrophages
 1036 C. Production of interferon-gamma by T-helper cells
 1037 D. Migration of T-helper cells to the lungs

1038 Please respond in the following format: '##Explanation:\n[explanation]\n\n##Answer:\n[option]'
 1039

1040 **Output:**

1041 <think> *#reasoning trajectory*

1042 Okay, let's tackle this question step by step. The patient is a 55-year-old nurse who recently
 1043 returned from India and has symptoms of TB. Let's break down the information given.

1044 She had a tuberculin skin test (TST) three months ago with 3 mm induration, which is considered
 1045 negative (since the cutoff for healthcare workers is usually 10 mm). Now, she has a positive
 1046 sputum culture for acid-fast bacilli, which points to active tuberculosis. The chest X-ray shows
 1047 hilar lymphadenopathy, which is common in primary TB, especially in the right side.

1048 The question is asking about the first immunologic process that occurred. The options are about
 1049 the sequence of immune responses when someone is infected with *Mycobacterium tuberculosis*.

1050 So, the initial step when TB bacteria enter the body is inhalation. The bacilli reach the alveoli,
 1051 where they are taken up by alveolar macrophages. However, *M. tuberculosis* has mechanisms
 1052 to survive inside these macrophages. The bacteria can replicate within the macrophages until
 1053 the macrophages are overwhelmed and lyse, releasing more bacteria. This replication within
 1054 macrophages is an early step before the immune system starts to respond more effectively.

1055 After that, the adaptive immune response kicks in. T-helper cells (CD4+ T cells) migrate to the site
 1056 of infection. These cells release cytokines like interferon-gamma, which activate macrophages
 1057 to become more effective at killing the bacteria. The activated macrophages form granulomas
 1058 (tubercles) to contain the infection. The formation of the granuloma is part of the body's attempt
 1059 to wall off the infection.

1060 So the sequence would be: bacteria enter macrophages and replicate (B), then T-cells migrate
 1061 (D), produce interferon-gamma (C), leading to granuloma formation (A).

1062 The question asks which happened first. So the first step after exposure would be the replication
 1063 within macrophages. The TST was negative before her trip, suggesting she wasn't previously
 1064 infected. Now she's positive, so this is a new infection. The initial infection's first immunologic
 1065 process is the bacteria replicating in macrophages before the immune response starts.

1066 </think>

1067 <answer> *#answer*

1068 ##Explanation:

1069 The patient's recent exposure and subsequent active tuberculosis indicate a new infection. The initial
 1070 immunologic process begins when *Mycobacterium tuberculosis* is inhaled and phagocytosed
 1071 by alveolar macrophages. The bacteria survive and replicate within these macrophages (option
 1072 B), which occurs before the adaptive immune response. Subsequent steps include T-helper cell
 1073 migration to the lungs (D), interferon-gamma production (C), and granuloma formation (A). The
 1074 replication within macrophages is the earliest event in the immunologic cascade.

1075 ##Answer:

1076 B

1077 </answer>

1080
1081
1082
1083
1084
1085
1086
1087
1088
1089
1090
1091
1092
1093
1094
1095
1096
1097
1098
1099
1100
1101
1102
1103
1104
1105
1106
1107
1108
1109
1110
1111
1112
1113
1114
1115
1116
1117
1118
1119
1120
1121
1122
1123
1124
1125
1126
1127
1128
1129
1130
1131
1132
1133
Table 8: **An example of seed data in GSM8K distilled from DeepSeek-R1.****System Prompt:**

You are a helpful AI Assistant that provides well-reasoned and detailed responses for the math word problems. You first think about the reasoning process as an internal monologue and then provide the user with the concise and accurate answer. The final answer should be provided in the `\boxed{ }` .

Instruction:

John starts at an elevation of 400 feet. He travels downward at a rate of 10 feet down per minute for 5 minutes. What is his elevation now?

Output:

<think> `#reasoning trajectory`

Okay, so I need to figure out John's elevation after he travels downward for 5 minutes at a rate of 10 feet per minute. Let me start by understanding the problem. John starts at 400 feet, and he's moving downward. Moving downward would decrease his elevation, right? So, he's going from higher elevation to lower.

First, I should note his starting point: 400 feet. Then, he's going down at 10 feet per minute for 5 minutes. So, I think I can calculate the total distance he descended by multiplying the rate by the time. That makes sense because if you go 10 feet every minute, then in 5 minutes, that's $10 * 5 = 50$ feet. Wait, yes, so he would have gone down 50 feet in total.

Since he's moving downward, his new elevation will be the original elevation minus that descent. So, subtracting 50 feet from 400 feet. Let me do that calculation: $400 - 50$. That gives 350 feet. Hmm, so his elevation after 5 minutes should be 350 feet.

Wait, let me check that again. Multiplication first: 10 feet per minute times 5 minutes is indeed 50 feet. Then subtract that from the starting elevation. Yeah, 400 minus 50 is 350. I think that's correct. Maybe I should visualize this. Imagine he's on a hill at 400 feet. Each minute, he goes down 10 feet, so after 1 minute, he's at 390, then 380, 370, 360, 350 after 5 minutes. Each step is 10 feet lower. So yes, five steps would be 50 feet total.

Is there any chance I might have mixed up the direction? Like thinking he's ascending? But the problem clearly states he's traveling downward. So subtracting is the right operation. Okay, I feel confident that this is right. Let me just go through the steps again to confirm. Starting elevation 400. Rate: 10 ft/min downward. Time: 5 min. Total descent is rate * time = $10*5=50$ ft. New elevation: $400 - 50 = 350$ ft. Yeah, that checks out. I think that's the correct answer.

</think>

`#answer`

John starts at an elevation of **400 feet**.

To find his elevation after descending:

1. **Calculate total descent**: Rate = 10 feet/minute \times 5 minutes = **50 feet**.
2. **Subtract the descent from the starting elevation**: $400 \text{ feet} - 50 \text{ feet} = **350 \text{ feet}**$.

Verification: Each minute, his elevation decreases by 10 feet:

- After 1 minute: $400 - 10 = 390$ feet
- After 2 minutes: $390 - 10 = 380$ feet
- Continuing this pattern for 5 minutes leads to **350 feet**.

Final Answer:

`\boxed{350}`

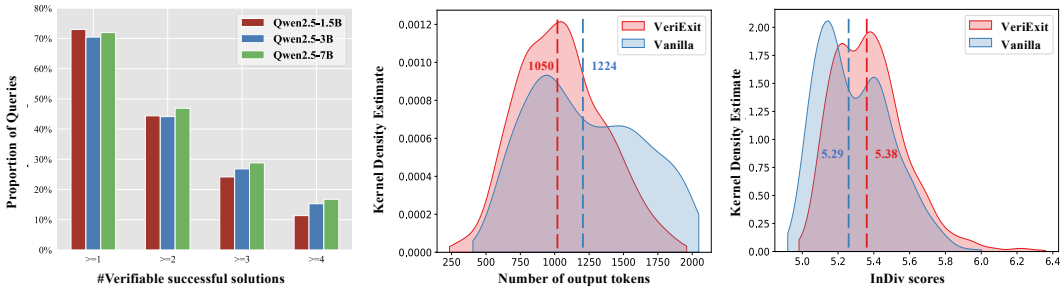


Figure 5: **Left:** Coverage of verifiable successful solutions. The x-axis denotes the number of verifiable successful solutions in a query. **Middle:** Distribution of the number of output tokens of correct self-generated solutions. **Right:** Distribution of *InDiv* scores of correct self-generated solutions. In the middle and right sub-figures, we use the initial SFT Qwen2.5-1.5B models.

C MORE EXPERIMENTS AND ANALYSES

C.1 ANALYSIS OF *VeriExit* SAMPLING STRATEGY

Reliability of *VeriExit*. In HSIR, we propose *VeriExit* to efficiently collect more successful solutions for difficult queries by reusing partial correct reasoning steps of previous failed solutions. Here, to verify the reliability of this idea, we calculate the coverage of these verifiable successful solutions, which contain intermediate reasoning steps that arrived at the correct answer. Figure 5 (Left) illustrates the coverage of these solutions in the most difficult queries of MedQA. Specifically, we refer to the queries that did not obtain any correct solutions during the K -times ($K = 10$ in our experiments) self-generation processes as the most difficult ones. The x-axis denotes the number of verifiable successful solutions in a query, and the y-axis denotes the proportion of queries. As seen, among all Qwen2.5 family models, nearly 70% of these most difficult queries have at least one verifiable successful solution, and more than 10% of these queries have 4 or more verifiable successful solutions. We believe that in the simpler queries, there is a larger proportion of previous failed solutions that can be converted into verifiable successful solutions by *VeriExit*. These results can demonstrate the reliability of our *VeriExit* Sampling Strategy.

Moreover, we compare the solutions resampled by *VeriExit* and the previous correct solutions. In practice, we measure the length and *InDiv* scores of solutions on the difficult MedQA queries (obtaining four correct solutions during the previous self-generation) generated by initial SFT Qwen2.5-1.5B models, and visualize the distributions in Figure 5 (Middle and Right). As seen, compared to the previous correct solutions generated by the vanilla sampling strategy, our *VeriExit* can sample shorter and concise reasoning trajectories. We attribute it to the self-truncation and early-exit processes of *VeriExit*, which can skip the redundant and repetitive reasoning steps. This can also explain why the “-w/ *VeriExit*” method in Table 3 can improve reasoning efficiency against the ReST^{EM}.

More *VeriExit* variants. The core of our *VeriExit* is to determine whether the reasoning step has reached the ground-truth answer. There are several methods to achieve this goal. Specifically, the simplest approach is to directly match the text between the reasoning output and the ground-truth answer. If the reasoning output explicitly mentions the answer, *e.g.*, “answer is $\{y_i\}$ ”, we can assume that it arrives at the ground-truth answer. Beyond this simple heuristic, inspired by SelfCheckGPT (Manakul et al., 2023), we can further use two more sophisticated approaches: **NLI-based** and **prompt-based**. In the **NLI-based** *VeriExit*, we use an external Natural Language Inference (NLI) model to judge the relationships between the reasoning output and answer. The NLI model can determine whether the reasoning output entails the answer according to the similarity of sentence representations, *i.e.*, $\mathbb{I}(\text{NLI}(\hat{r}_{i,l}^k, y_i) = \text{entailment})$. In practice, we use the powerful DeBERTa-v3-large-mnli⁸ as the NLI model. In the **prompt-based** *VeriExit*, we query the current \mathcal{M}_{t-1} to assess whether the reasoning output and answer convey the same meaning by using the following prompt: “*You are a semantic-equivalence classifier. Your only goal is to decide whether the two input sentences convey the same meaning. Please direct output the answer following the*”

⁸<https://huggingface.co/MoritzLaurer/DeBERTa-v3-large-mnli-fever-anli-ling-wanli>

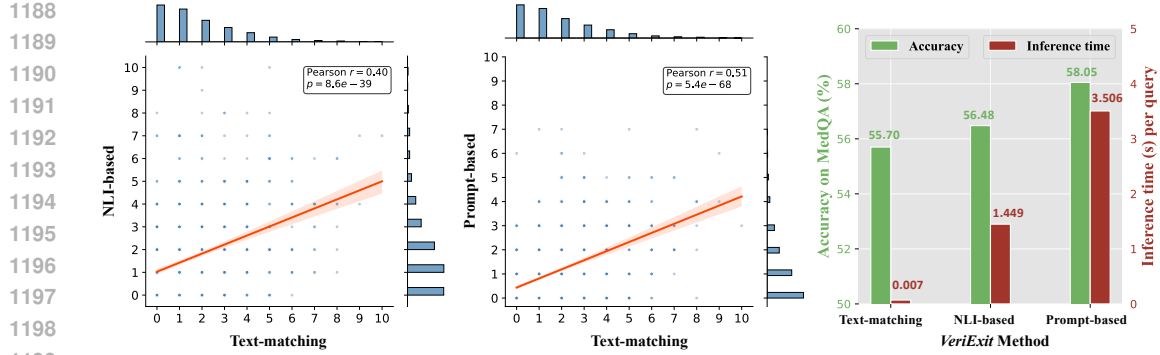


Figure 6: **Left:** Correlation between text-matching and NLI-based *VeriExit* methods. **Middle:** Correlation between text-matching and prompt-based *VeriExit* methods. **Right:** Performance and efficiency comparisons of HSIR-SFT variants equipped with different *VeriExit* methods. In the left and middle sub-figures, the axes denote the number of verifiable successful solutions per query. Qwen2.5-3B model is used in this experiment and all models are self-improved for one iteration.

format: ‘##Answer: [YES|NO|UNCLEAR]’’. Notably, for both methods, we convert the answer into a full sentence using the template “the answer is y_i ” to ensure consistent semantic comparison.

To evaluate different *VeriExit* strategies, we measure the coverage of verifiable successful solutions on the most difficult queries of MedQA using each strategy. Using the text-matching method as the baseline, we illustrate the correlation between text-matching and NLI-based/prompt-based methods in Figure 6 (Left) and (Middle), respectively. In this experiment, we use the Qwen2.5-3B as the base model. The results show that text-matching *VeriExit* correlates well with both alternative methods, with Pearson Correlation Coefficients exceeding 0.4 and p-values below 0.05, indicating that all *VeriExit* variants produce largely consistent predictions. Further, we replace the *VeriExit* strategy in the HSIR-SFT framework, and compare the performance and efficiency of HSIR-SFT variants in Figure 6 (Right). The findings are as follows: 1) both NLI-based and prompt-based methods achieve better reasoning performance, as they can more accurately identify the correct reasoning steps during *VeriExit*; 2) although effective, these methods incur more additional inference overhead. Therefore, for simplicity and efficiency, we use the text-matching method in our work by default.

C.2 ANALYSIS OF *InDiv* SCORE

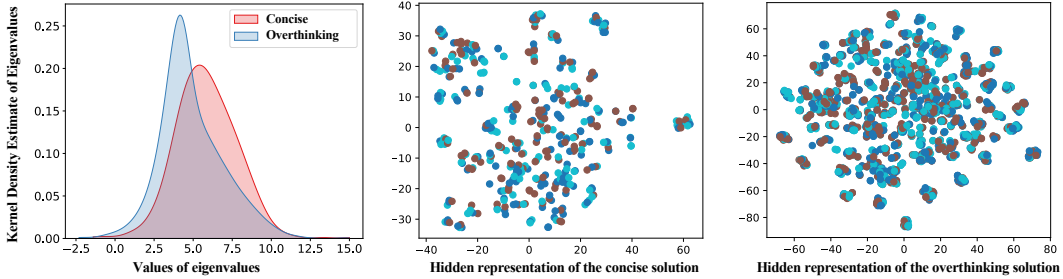


Figure 7: **Left:** Distribution of eigenvalues of hidden representation in the concise and overthinking solutions. **Middle:** t-SNE visualizations of hidden representations in the concise solution. **Right:** t-SNE visualizations of hidden representations in the overthinking solution. Here, we use the initial SFT Qwen2.5-1.5B as the test model. The concise and overthinking solutions are from Table 15.

Correlation between *InDiv* scores and semantic entropy. Here, we investigate the correlation between our *InDiv* scores and the semantic entropy of hidden representations \mathbf{H} . First, we introduce the **Matrix-Based Entropy** (Giraldo et al., 2014; Skean et al., 2023; 2025), which is a famous information-theoretic quantity. For the cross-covariance matrix $\Sigma_i^k = \mathbf{H}_i^{k\top} \cdot \mathbf{J}_d \cdot \mathbf{H}_i^k$ and its

1242 eigenvalues $\{\lambda_{i,u}^k\}_{u=1}^m$, the matrix-based entropy of order $\alpha > 0$ is:
 1243

$$1244 \quad 1245 \quad \mathbf{S}_{\alpha,i}^k(\mathbf{H}_i^k) = \frac{1}{1-\alpha} \log \left[\sum_{u=1}^m \left(\frac{\lambda_{i,u}^k}{\text{Tr}(\mathbf{H}_i^k)} \right)^\alpha \right], \quad (11)$$

1246 where $\text{Tr}(\cdot)$ denotes the trace operator obtained from the sum of α -power of each eigenvalues (Horn
 1247 & Johnson, 2012). When $\alpha \rightarrow 1$, the entropy $\mathbf{S}_{\alpha,i}^k(\mathbf{H}_i^k)$ corresponds to the Shannon's entropy of
 1248 hidden representations. Intuitively, if the eigenvalues of \mathbf{H} are in a uniform distribution, the entropy
 1249 will be higher, indicating that \mathbf{H} contains more diverse features (Skean et al., 2025). Conversely,
 1250 if the eigenvalues collapse to a small area, the entropy will be smaller. To verify it, we compare
 1251 the distributions of eigenvalues between the concise and overthinking solutions identified by our
 1252 *InDiv* scores. Specifically, we directly use the solutions in Table 15, and illustrate their eigenvalue
 1253 distributions in Figure 7 (Left). It can be found that the eigenvalue distributions of the concise
 1254 solution are more uniform than those of the overthinking solution. To have a closer look, we directly
 1255 visualize the hidden representations of both solutions. Figure 7 (Middle) and (Right) show the t-SNE
 1256 results of the concise and overthinking solutions, respectively. We can observe that the distribution
 1257 of hidden representations of the concise solution is more diverse and uniform, while that of the
 1258 overthinking solution is more similar and concentrated. Overall, these results indicate that a higher
 1259 *InDiv* score usually refers to a higher semantic entropy of hidden representations, which effectively
 1260 proves why our *InDiv* score can help identify overthinking solutions.
 1261

1262 Impact of layer depth for calculating *InDiv* 1263 scores.

1264 As mentioned in §3.2, we use the hidden
 1265 representations from the middle layer of
 \mathcal{M}_{t-1} to calculate the *InDiv* scores. Here, we
 1266 investigate the impact of different layer depths
 1267 by comparing the performance of Qwen2.5-1.5B
 1268 models trained with different HSIR-SFT con-
 1269 figurations on MedQA. Specifically, since the
 1270 Qwen2.5-1.5B contains 28 layers, we vary the
 1271 layer used for calculating *InDiv* scores across $\{5, 10, 15, 20, 25\}$ and illustrate the comparative re-
 1272 sults in Figure 8. For reference, we also include
 1273 the results of SFT-Initial and ReST^{EM} methods.
 1274 All models are self-improved for one iteration.
 1275 As seen, HSIR-SFT with varied layer depth can
 1276 consistently outperform the other baseline meth-
 1277 ods, indicating that HSIR is relatively robust
 1278 to the choice of layer. Moreover, when using
 1279 the middle layer (*i.e.*, 15-th layer), HSIR-SFT
 1280 achieves the best performance. We conjecture that the middle layer encodes richer and more useful
 1281 semantic information (Skean et al., 2025; Azaria & Mitchell, 2023; Liu et al., 2019), thus resulting in
 1282 more accurate *InDiv* scores. Based on these observations, we choose to adopt the middle layer of
 \mathcal{M}_{t-1} for calculating *InDiv* scores in this work.
 1283

1284 **More ablation study in *InDiv*.** There
 1285 are two important strategies in our *InDiv*:
 1286 attention-aware weighting mechanism and
 1287 *InDiv* normalization. The former is to ob-
 1288 tain more fine-grained intrinsic diversity,
 1289 while the latter is to regularize the *InDiv*
 1290 score for more flexible data filtering. To
 1291 evaluate their contributions, we compare
 1292 our full HSIR-SFT with two variants: 1)
 1293 “-w/o attention-aware”, which removes the
 1294 attention-aware weighting mechanism, *i.e.*,
 $1295 \text{Atten}_{i,u}^k = \frac{1}{m}$ in Eq. 5; 2) “-w/o nor-
 1296 malization”, which directly uses the InDiv_i^k in Eq. 5 as the final score and filters the solutions with
 1297 lower scores within each query. Notably, The filtering ratio is adjusted to ensure that both variants
 1298



Figure 8: **Analysis of different layer depths for calculating *InDiv* scores.** Notably, we use the Qwen2.5-1.5B (with a total of 28 layers) as the test model. All models are trained for one self-improvement iteration.

Table 9: **Analysis of important components in *InDiv*.** All models are self-improved for one iteration.

Method	Qwen2.5-1.5B		Qwen2.5-3B	
	MedQA	GSM8K	MedQA	GSM8K
SFT-Initial	38.10	63.99	49.02	77.18
HSIR-SFT	45.33	71.72	55.70	86.13
-w/o attention-aware	45.20	71.34	55.38	85.75
-w/o normalization	43.52	71.27	54.13	85.60

use approximately the same amount of training data as the original HSIR-SFT. Table 9 presents the results, showing that removing either strategy leads to performance degradation. These findings consistently demonstrate the effectiveness of both strategies.

C.3 PARAMETER ANALYSIS

Effect of τ . The threshold τ , used to filter the overthinking solutions, is an important hyperparameter in our HSIR. In this study, we analyze its influence by evaluating the performance with different τ values, spanning from -0.75 to 0.75. Figure 9 illustrates the comparative results of Qwen2.5-3B models trained with HSIR-SFT on MedQA and GSM8K. For reference, we also report the results without data filtering as the baseline. As seen, compared to the baseline, HSIR with suitable τ can generally achieve better performance, showing the effectiveness of using *InDiv* scores to filter overthinking solutions. However, too large τ (*i.e.*, 0.75) would lead to performance degradation, as many helpful training samples might be ignored. HSIR performs best with $\tau = -0.5$, thus leaving as our default experimental settings.

Effect of J . The hyperparameter J , which is used to control the sample count of recycled solutions during *VeriExit*, is also important for our HSIR. Here, to investigate its impact, we evaluate our HSIR-SFT with different J values ranging from 1 to 7. The comparative results of Qwen2.5-1.5B on MedQA are illustrated in Figure 10. For reference, we also include the results of SFT-Initial and ReST^{EM}. All models are self-improved for one iteration. From these results, we find that: 1) When J is too small (*e.g.*, $J = 1$), our *VeriExit* struggles to sample enough correct solutions, limiting the effectiveness of HSIR-SFT. 2) When J is too large (*e.g.*, $J = 7$), many sampled solutions share similar prefix reasoning steps, reducing the diversity of training data and leading to sub-optimal performance. 3) Across all J values, our HSIR-SFT consistently outperforms the baseline methods, proving its robustness. Notably, in the case of $J = 5$, HSIR-SFT achieves the best performance. Thus, we use it as the default setting in this work.

C.4 IMPACT OF SEED DATA

Seed data from QWQ-32B. As mentioned in §2.1, we first fine-tune the base model \mathcal{M}_{base} on the seed dataset \mathcal{S} to make it have basic long-CoT reasoning abilities. Intuitively, high-quality seed data can improve the basic reasoning ability of LRM and boost the effectiveness of self-improvement training. To verify it, we replace the seed data used in our main experiments with that distilled from QWQ-32B⁹. Taking the MedQA as an example, we fine-tune the Qwen2.5 family models on the seed data distilled from QWQ-32B and self-generated pseudo-labeled data for one iteration, using different self-improvement training methods. Table 10 reports the average accuracy and number of output tokens of all tuned models, from which we find that: (1) Compared to the seed data distilled from DeepSeek-R1, the seed data generated by QWQ-32B performs differently in different models. For the smaller models (*i.e.*, Qwen2.5-1.5B), the seed data from QWQ-32B brings more performance

⁹<https://qwenlm.github.io/blog/qwq-32b-preview/>

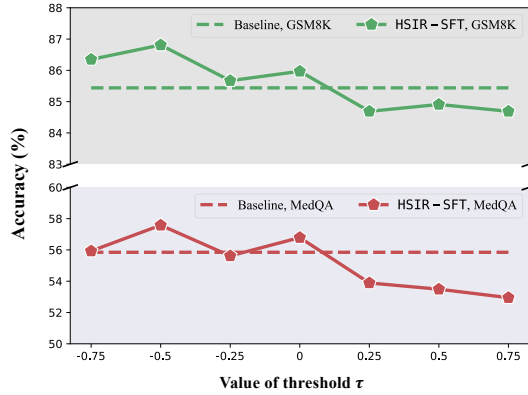


Figure 9: **Analysis of threshold τ .** “Baseline” means that we do not filter the overthinking solutions, *i.e.*, removing the *InDiv* in HSIR.

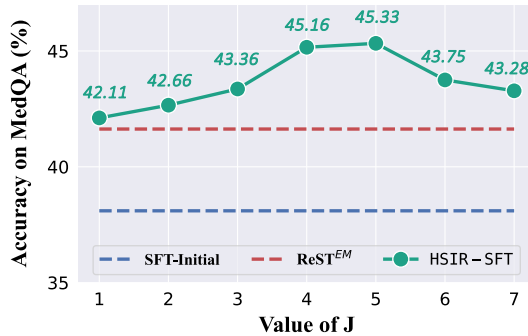


Figure 10: **Analysis of sampling count J .** We use the Qwen2.5-1.5B as the test model. All models are trained for one self-improvement iteration.

3) Across all J values, our HSIR-SFT consistently outperforms the baseline methods, proving its robustness. Notably, in the case of $J = 5$, HSIR-SFT achieves the best performance. Thus, we use it as the default setting in this work.

1350 gains. Conversely, for the larger 7B model, it leads to worse results. We conjecture that there is a large
 1351 capacity gap between Qwen2.5-1.5B and DeepSeek-R1, while using a smaller QWQ-32B as a teacher
 1352 can achieve a smooth knowledge transfer (Mirzadeh et al., 2020; Zhang et al., 2023). However, for the
 1353 Qwen2.5-7B, a smaller teacher model might struggle to provide sufficient knowledge, thus leading
 1354 to suboptimal performance. (2) When using the seed data generated by QWQ-32B, our HSIR can
 1355 still outperform the other baseline methods and achieve better reasoning performance and efficiency.
 1356 These results demonstrate the universality and robustness of HSIR.

1357
 1358 **Table 10: Performance comparison of the seed data distilled from different LRM**s. We evaluate
 1359 the Qwen2.5 models fine-tuned with different self-improvement SFT methods for one iteration.

Methods	Train	Qwen2.5-1.5B		Qwen2.5-3B		Qwen2.5-7B		Overall	
		Avg.	MedQA	Tokens	MedQA	Tokens	MedQA	Tokens	Accuracy
<i>Seed data distilled from DeepSeek-R1</i>									
SFT-Initial	1.0K	38.10	1,779	49.02	1,644	62.45	1,428	49.86	1,617
<i>Seed data distilled from QWQ-32B</i>									
SFT-Initial	1.0K	40.22	1,677	50.04	1,569	61.12	1,607	50.46	1,618
SFT-Oracle	8.0K	43.99	1,781	60.25	1,451	69.13	1,419	57.79 ^{↑7.33}	1,550 ^{↓4.2%}
STaR	4.9K	39.35	1,576	49.25	1,500	61.82	1,541	50.14 ^{↓0.32}	1,539 ^{↓4.9%}
ReST ^{EM}	37.9K	44.38	1,431	54.77	1,307	65.43	1,401	54.86 ^{↑4.40}	1,380 ^{↓14.7%}
HSIR-SFT	29.6K	46.58	1,167	55.70	1,192	66.93	1,266	56.40^{↑5.94}	1,208^{↓25.3%}

1371 **Is the seed data from a frontier model**
 1372 **necessary?** In the above experiments, we
 1373 empirically find that initial LRM trained
 1374 with high-quality seed data can effectively
 1375 self-improve via our HSIR. Here, we con-
 1376 duct more in-depth experiments to investi-
 1377 gate whether the seed data distilled from
 1378 a frontier model is necessary. Specifically,
 1379 we focus on two types of seed data: 1) **low-**
 1380 **quality seed data**, which is distilled from a
 1381 smaller and weaker LRM; 2) **self-distilled**
 1382 **seed data**, which is generated by the model
 1383 itself via an in-context learning approach. Using the Qwen2.5-3B as the testbed, we obtain low-quality
 1384 seed data from the SFT-Initial Qwen2.5-1.5B. For the self-distilled seed data, we randomly select
 1385 three examples distilled from DeepSeek-R1 as few-shot demonstrations and use them to guide the
 1386 base Qwen2.5-3B for generating the seed data. Notably, for all methods, we use the same queries x_i
 1387 and sample a correct solution for each query, ensuring the same number of training samples across
 1388 seed data types. Qwen2.5-3B model is first fine-tuned on different seed data, and then self-improved
 1389 with various SFT approaches for one iteration. Table 11 presents the comparative results of different
 1390 Qwen2.5-3B models on MedQA. From it, we observe that: 1) the quality of seed data is critical, as
 1391 initial SFT on low-quality seed data significantly degrades performance; 2) across all seed data types,
 1392 our HSIR consistently brings performance gains, further validating its effectiveness. In general,
 1393 while it is feasible for an LLM to self-distill seed data and subsequently self-improve using HSIR,
 1394 leveraging more high-quality seed data from stronger frontier models allows HSIR to realize its full
 1395 potential and achieve better performance.

C.5 WHEN GROUND-TRUTH ANSWER ARE UNAVAILABLE

1397 Following many prior studies (Zelikman et al., 2022; Yuan et al., 2023; Wang et al., 2024; Pang et al.,
 1398 2024), we assume that the ground-truth answers of unlabeled dataset \mathcal{D} are available in this work.
 1399 Some readers may wonder how our HSIR performs when ground-truth answers are unavailable in
 1400 some scenarios. Actually, in this setting, we can follow Huang et al. (2023) and use the majority-voting
 1401 answer among multiple candidate solutions as a pseudo answer, i.e., $\tilde{y}_i = \arg \max_{\tilde{y}_i^j} \sum_{k=1}^K \mathbb{I}(\tilde{y}_i^j =$
 1402 $\tilde{y}_i^k)$. Here, the \tilde{y}_i is denoted as the self-consistency pseudo label. Although the \tilde{y}_i may be incorrect,
 1403 we can still apply our HSIR to improve the LRM as described in §3. To verify its effectiveness, we
 1404 evaluate it on several Qwen2.5 models and report the results in Table 12. For reference, we use the

ReST^{EM} as the baseline method, and also include the results based on ground-truth answers. As seen, using the self-consistency pseudo labels indeed yields slightly sub-optimal results compared to ground-truth answers. Nevertheless, our HSIR-SFT method still achieves substantial improvements, with an average gain of +6.14%, proving that HSIR remains effective even in unlabeled scenarios.

Table 12: **Performance comparison of Qwen2.5 models on MedQA and GSM8K benchmarks.** Notably, “SC →” refer to using the majority-voting answer among multiple candidate solutions of SFT-Initial models as the pseudo labels of \mathcal{D} . All models are self-improved for one iteration.

Methods	Qwen2.5-1.5B		Qwen2.5-3B		Qwen2.5-7B		Overall	
	MedQA	GSM8K	MedQA	GSM8K	MedQA	GSM8K	Accuracy	Tokens
SFT-Initial	38.10	63.99	49.02	77.18	62.45	83.93	62.45	1,536
<i>Using ground-truth answers</i>								
ReST ^{EM}	41.63	69.75	55.22	83.95	64.18	88.17	67.15 ^{↑4.70}	1,268 _{↓17.5%}
HSIR-SFT	45.33	71.72	55.70	86.13	67.32	88.78	69.16_{↓6.71}	1,075 _{↓30.0%}
<i>Using self-consistency pseudo labels</i>								
SC → ReST ^{EM}	40.46	70.36	51.69	83.70	64.57	87.04	66.30 _{↓3.85}	1,322 _{↓13.9%}
SC → HSIR-SFT	44.78	71.72	54.99	84.69	65.91	89.46	68.59_{↓6.14}	1,108 _{↓27.8%}

C.6 RESULTS IN HIGH-RESOURCE SCENARIOS

In our work, we assume that only a small amount of seed data is available. Some readers may wonder whether our HSIR method remains effective in high-resource scenarios, where sufficient seed data is provided. To verify it, we use all training samples distilled from DeepSeek-R1 as the seed data to initially fine-tune the base model, *i.e.*, using the SFT-Oracle in Table 1 as the \mathcal{M}_0 . Table 13 presents the results of Qwen2.5-1.5B and Qwen2.5-3B models on MedQA. For reference, we also report the results of ReST^{EM} and IRPO as baselines. All models are self-improved for one iteration. From these results, we find that both HSIS-SFT and HSIS-DPO methods can effectively improve the performance and inference efficiency of SFT-Oracle models. Specifically, with the help of HSIS-DPO, Qwen2.5-3B model achieves +7.93% performance gain on MedQA. These findings demonstrate that our HSIS has great potential to enhance the self-improvement capabilities of fully-trained and powerful LMRs.

C.7 EFFICIENCY OF HSIR

Some readers may be concerned about the efficiency of our HSIR method, as it requires additional forward passes of LMRs. Actually, during the *VeriExit* sampling phase, we only sample the final answer without regenerating intermediate reasoning trajectories, making it much faster than simply allocating more trials to failed queries. In our preliminary experiments, we found that the *VeriExit* sampling can be completed in [an average of one hour on 8 NVIDIA A800 \(80GB\) GPUs](#), which is about 1/4 of the time required for generating full reasoning trajectories. On the other hand, to obtain the *InDiv* scores, the query and its solution are fed into the model in a teacher-forcing manner, requiring only a single forward pass and introducing minimal latency. In practice, during HSIR-SFT and HSIR-DPO training, obtaining hidden states for each token introduces some computational overhead, but this can be completed in about half an hour on 8 NVIDIA A800 (80GB) GPUs. Moreover, during the H-GRPO training, we can reuse the hidden representation obtained by the reference model without extra forward passes. The actual computation of the InDiv score itself is lightweight, involving only simple vector operations that take a few seconds. More importantly, owing to the data filtering process of HSIR, the training budget can be significantly reduced, *e.g.*, from 53.6K to 38.8K during fine-tuning Qwen2.5-1.5B at the last iteration. In general, the inference latency of HSIR is tolerable against its performance gains.

1458 C.8 MORE SELF-IMPROVEMENT ITERATIONS
1459

1460 Due to limited computation resources, we set
1461 the maximum self-improvement iterations T to
1462 3 in the main experiments. Here, to further in-
1463 vestigate whether additional iterations can im-
1464 prove performance, we extended the maximum
1465 training iterations T from 3 to 5, and compare
1466 the MedQA accuracy of Qwen2.5-1.5B mod-
1467 els trained with different self-improvement SFT
1468 training methods across the iterations. Figure 11
1469 illustrates the comparative results, from which
1470 we observe that: 1) With the increase of self-
1471 improvement training iterations, both STaR and
1472 ReST^{EM} exhibit a trend where performance ini-
1473 tially improves but then declines, which is sim-
1474 ilar to the findings of Ding et al. (2025). This
1475 may be due to overfitting on easy-to-learn sam-
1476 ples. Conversely, by mitigating the data imbal-
1477 ance problem, our HSIR can collect more chal-
1478 lenging samples and achieve continuous per-
1479 formance improvements. 2) As self-improvement training progresses, the performance gains of HSIR
1480 tend to be smaller, indicating the existence of an upper-bound for self-improvement training.

1480 C.9 COMPATIBILITY WITH SELF-CONSISTENCY
1481

1482 The goal of our work is to propose a self-
1483 improvement training framework that unlocks
1484 the internal long-CoT reasoning capabilities of
1485 LRM, rather than to optimize inference. There-
1486 fore, in the main experiments, we do not com-
1487 pare HSIR with inference-time methods, such
1488 as Self-Consistency (SC) (Wang et al., 2023).
1489 Nevertheless, given that SC is widely used to en-
1490 hance LRM reasoning performance, we include
1491 it in this experiment. Specifically, during infer-
1492 ence, we sample five solutions from the model
1493 and select the majority-vote answer as the pre-
1494 diction. Figure 12 shows the comparative results
1495 of Qwen2.5 models on MedQA, where “-w/ SC”
1496 means using the SC method. As seen, increasing
1497 the test-time compute through SC improves the
1498 reasoning performance of SFT-Initial models ef-
1499 fectively. However, it still underperforms our
1500 HSIR-SFT method, even if HSIR-SFT only samples a single solution during inference. More
1501 encouragingly, combining the HSIR-SFT and SC methods consistently yields further performance
1502 improvements. For instance, for the Qwen2.5-3B model, with the help of SC, HSIR-SFT achieves a
1503 12.25% performance gain over the SFT-Initial model. These results prove the compatibility of our
1504 HSIR with inference-time SC method.

1504 C.10 CASE STUDY
1505

1506 To have a closer look, we provide some cases in this part. Specifically, Table 14 shows the comparison
1507 of self-generated solutions between before and after using our *VeriExit* sampling strategy. We show
1508 the self-generated results of Qwen2.5-1.5B on the MedQA task. As seen, in the previous failed
1509 solutions, the model indeed arrived at the correct answer during intermediate reasoning steps, yet
1510 ultimately failed to produce the accurate outcome due to reasoning deviation. Conversely, by using
1511 our verify-then-exit strategy, we can convert it into a collect solution. Table 15 shows the comparison
of *InDiv* scores between concise and overthinking self-generated solutions. Obviously, *InDiv* scores

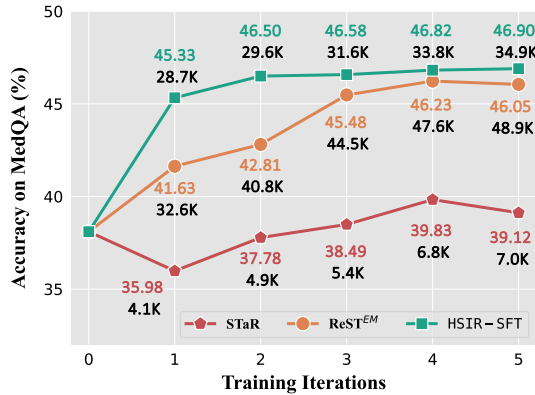


Figure 11: **Results of Qwen2.5-1.5B models training for more self-improvement iterations.** Here, we report both test accuracy and the number of training samples on MedQA.

Figure 11: **Results of Qwen2.5-1.5B models training for more self-improvement iterations.** Here, we report both test accuracy and the number of training samples on MedQA.

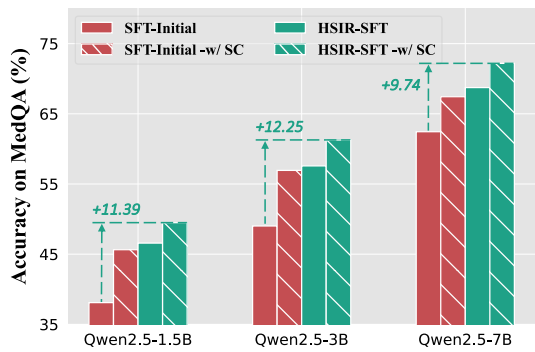


Figure 12: **Performance comparison between with and without the self-consistency method.** Notably, we report the results of HSIR-SFT after three self-improvement iterations.

Figure 12: **Performance comparison between with and without the self-consistency method.** Notably, we report the results of HSIR-SFT after three self-improvement iterations.

1512 can reflect the redundancy and repetitiveness of reasoning steps generated by Qwen2.5-1.5B on the
 1513 MedQA task. We observe that the overthinking solution indeed obtains a much lower *InDiv* score.
 1514 These case studies support the intuition and soundness of our proposed methods.

1515 Table 16 and Table 17 show the comparison of reasoning results of Qwen2.5-7B models before
 1516 and after training using HSIR on MedQA and GSM8K test sets, respectively. It can be found that,
 1517 with the help of HSIR, the model can reason more accurately and concisely, thus resulting in better
 1518 performance. These case studies prove the effectiveness of HSIR.

1519
 1520 **Table 14: An example of converting the failed solution into the correct one via the *VeriExit***
 1521 **strategy.** In this case from MedQA, the ground-truth answer is “D”. As seen, the failed solution
 1522 arrived at the correct answer during intermediate reasoning steps (highlighted in green), but diverted
 1523 into an incorrect one due to overly backtracking (highlighted in red).

1524
 1525 **Previous Failed Solution:**

1526 <think>

1527 Okay, let's try to work through this question.

1528 ...

1529 So, if the options include allopurinol (option C), then that's the answer. But the options given
 1530 here are D. Xanthine oxidase inhibitor. Wait, but xanthine oxidase inhibitors are allopurinol and
 1531 other drugs like febuxostat. So, allopurinol is a xanthine oxidase inhibitor. So, if the answer is C,
 1532 then allopurinol. But the question is asking for the long-term treatment. **So, if the options don't**
 1533 **include allopurinol, then perhaps the answer is D.** **Wait**, I think the answer is C. Allopurinol. So,
 1534 the correct answer would be C.

1535 ...

1536 ##Answer:

1537 C

1538 </answer>

1540 **New Solution Generated by *VeriExit*:**

1541 <think>

1542 Okay, let's try to work through this question.

1543 ...

1544 So, if the options include allopurinol (option C), then that's the answer. But the options given
 1545 here are D. Xanthine oxidase inhibitor. Wait, but xanthine oxidase inhibitors are allopurinol and
 1546 other drugs like febuxostat. So, allopurinol is a xanthine oxidase inhibitor. So, if the answer is C,
 1547 then allopurinol. But the question is asking for the long-term treatment. **So, if the options don't**
 1548 **include allopurinol, then perhaps the answer is D.**

1549 </think> (verify then exit)

1550 <answer>

1551 ...

1552 ##Answer:

1553 D

1554 </answer>

1556
 1557
 1558 **Table 15: Comparison of *InDiv* scores between concise and overthinking solutions in a single**
 1559 **query.** Here, we use the case of MedQA. Compared to the concise solution, the overthinking solution
 1560 contains more repetitive reasoning steps (highlighted in orange).

1561
 1562 **Concise Solution:**

1563 <think>

1564 Okay, let's try to figure this out. So the question is about malnutrition in children and which
 1565 amino acid is needed for them. The symptoms described are Kwashiorkor, which is protein
 deficiency. The options are A. Alanine, B. Tyrosine, C. Arginine, D. Methionine.

1566 First, I remember that kwashiorkor is typically due to inadequate protein intake. The main issue
 1567 is the lack of essential amino acids, especially the ones that the body can't make on its own.
 1568 The nine essential amino acids are tryptophan, threonine, histidine, lysine, isoleucine, leucine,
 1569 methionine, phenylalanine, and valine.

1570 Looking at the options, Methionine (D) is one of those essential amino acids. Alanine (A) is a
 1571 non-essential one, so maybe not needed here. Tyrosine (B) is an amino that's non-essential and
 1572 involved in protein synthesis but not for this presentation. Arginine (C) is also a non-essential
 1573 one and more associated with metabolic pathways like making creatine or proteins, not really for
 1574 this symptom. So the answer should be D. Methionine.

1575 </think>

1576 ...

1577 </answer>

1578 **InDiv Score: 5.99**

1580 **Overthinking Solution:**

1581 <think>

1582 Okay, let's tackle this question.

1583 ...

1584 So the answer would be D. Methionine. Wait, but I thought Tyrosine is an essential amino acid ...
 1585 So perhaps the answer is D. Methionine, because in some cases, the body uses up all the available
 1586 EAA's ...

1587 So the answer is D. Methionine. Because in kwashiorkor, without proper nutrition, the body
 1588 cannot utilize other amino acids. So supplementing with Methionine would help ...

1589 Therefore, the correct answer is D. Methionine. Because even if the diet has methionine, the
 1590 body can't utilize it. ...

1591 Alternatively, maybe the answer is Tyrosine. But I think not. So the answer is D.

1592 </think>

1593 ...

1594 </answer>

1595 **InDiv Score: 5.01**

1596 Table 16: Comparison of MedQA reasoning results of Qwen2.5-7B models before and after
 1597 training using HSIR. The ground-truth answer of this case is “D”.

1598 **Instruction:**

1599 For the following medical question, select one correct answer from A to D.

1600 *Question:* A 25-year-old African American man presents to his primary care provider for routine
 1601 blood work. He is a well-known case of sickle cell disease treated with hydroxyurea and tramadol
 1602 as needed for pain. He does not smoke or drink alcohol. The patient asks if his disease can
 1603 adversely affect his kidneys because his friend was recently diagnosed with end-stage renal
 1604 failure. Which of the following is a renal complication of sickle cell disease?

1605 *Options:*

- 1606 A. Membranous glomerulonephritis
- 1607 B. Proximal renal tubular acidosis
- 1608 C. Impaired urine diluting ability
- 1609 D. Impaired urine concentration ability

1610 **Output of SFT-Initial Model:**

1611 <think>

1612 Okay, let's tackle this question. So, the patient is a 25-year-old African American man with sickle
 1613 cell disease. He's on hydroxyurea and tramadol for pain. His friend has end-stage renal failure,
 1614 and he's asking if his disease can affect his kidneys. The question is about a renal complication
 1615 of sickle cell disease. The options are A to D.

1620 First, I need to recall the common renal complications associated with sickle cell disease. Sickled
 1621 cell disease can lead to various kidney issues. Let me think. The kidneys are affected because of
 1622 the hemolytic anemia and the high levels of hemoglobin S, which can cause microangiopathic
 1623 hemolysis.
 1624 Membranous glomerulonephritis (option A) is a type of nephrotic syndrome. I remember that
 1625 in sickle cell disease, membranous nephropathy is a known complication. It's an immune
 1626 complex-mediated process, leading to proteinuria and nephrotic syndrome. So that's a possibility.
 1627 Proximal renal tubular acidosis (option B) is a genetic disorder where the kidneys can't excrete
 1628 acids properly. But I don't think that's linked to sickle cell. PRSA is more about a defect in the
 1629 renal tubules' ability to handle acid, which isn't directly related to sickle cell's hemolysis.
 1630 Impaired urine diluting ability (option C) would be nephrogenic diabetes insipidus. That's when
 1631 the kidneys can't concentrate urine due to a defect in response to ADH. Again, not directly linked
 1632 to sickle cell. Maybe from other causes like certain drugs or genetic disorders.
 1633 Impaired urine concentration ability (option D) is nephrogenic diabetes insipidus as well. So this
 1634 is the same as option C. **So D is not the right answer here.**
 1635 So the options are between A and C. Wait, the question is about a renal complication. Sickled
 1636 cell can cause various issues. Let me think again. The patient's friend had end-stage renal failure,
 1637 which could be due to chronic kidney disease from sickle cell. The options given are specific
 1638 conditions.
 1639 Membranous glomerulonephritis (A) is a type of glomerular disease leading to nephrotic syn-
 1640 drome. In sickle cell, membranous nephropathy is a recognized complication, often presenting
 1641 with nephrotic syndrome. So A is a possible answer.
 1642 Impaired urine diluting ability (C) would be nephrogenic DI, which is unrelated. **So the correct**
 1643 **answer here is A. Membranous glomerulonephritis.** </think>
 1644 <answer>
 1645 ...
 1646 ##Answer:
 1647 A
 1648 </answer>

1651 **Output of HSIR-DPO Model:**

1652 <think>
 1653 Okay, let's tackle this question. So, the patient is a 25-year-old African American man with sickle
 1654 cell disease. He's on hydroxyurea and tramadol for pain. His friend had end-stage renal failure,
 1655 and the patient wants to know if his disease can affect his kidneys. The options are about different
 1656 renal complications.
 1657 First, I need to recall the common renal issues associated with sickle cell disease. Sickled
 1658 cell disease can cause various complications, including kidney problems. I remember that sickle cell
 1659 can lead to different glomerular diseases. For example, sickle cell nephropathy, which is a type
 1660 of glomerulonephritis. But looking at the options, option A is membranous glomerulonephritis. I
 1661 think that's more commonly associated with conditions like lupus or hepatitis B, but maybe I'm
 1662 mixing up. Alternatively, maybe it's a rare complication.
 1663 Wait, another possibility is that sickle cell can cause tubular issues. The options include proximal
 1664 renal tubular acidosis (option B). I know that sickle cell can lead to Fanconi syndrome, which is a
 1665 form of proximal tubular dysfunction. Fanconi syndrome includes glucosuria, aminoaciduria, etc.
 1666 But option B is specifically proximal RTA, which is a different condition. Proximal RTA is when
 1667 the proximal tubule can't reabsorb properly, leading to loss of nutrients and acidosis. But I'm not
 1668 sure if that's directly linked to sickle cell.
 1669
 1670
 1671
 1672
 1673

1674 Alternatively, the question might be pointing towards glomerular issues. The options include
 1675 impaired urine diluting ability (option C) and impaired concentration ability (option D). I remem-
 1676 ber that in sickle cell disease, there's a condition called hypernephrosis, which is an increase in
 1677 kidney size due to fluid overload. This can lead to dilutional hyponatremia because the kidneys
 1678 can't concentrate urine properly. **So, impaired concentration ability (option D) would be the issue**
 1679 **here**. But wait, the options are C and D as separate. Wait, impaired urine diluting ability—so the
 1680 kidneys can't excrete concentrated urine. Impaired concentration ability would be the opposite,
 1681 right? So in sickle cell, the kidneys might have trouble concentrating urine, leading to dilutional
 1682 hyponatremia. So option D would be the correct answer here.
 1683 But wait, another thought: sickle cell can cause glomerulonephritis leading to proteinuria,
 1684 hematuria, etc. But the options don't mention that. The options given are specific. **So, if the**
 1685 **question is about a renal complication, maybe the answer is D.**
 1686 </think>
 1687 <answer>
 1688 ...
 1689 ##Answer:
 1690 **D**
 1691 </answer>

1694 **Table 17: Comparison of GSM8K reasoning results of Qwen2.5-7B models before and after**
 1695 **training using HSIR.** The ground-truth answer of this case is “20”.

1696
 1697 **Instruction:**
 1698 Toby is reading a book that is 45 pages long. It averages 200 words a page. Toby can read at a
 1699 rate of 300 words per minute. He has to be at the airport in 60 minutes and plans to leave as soon
 1700 as he finishes the book. It takes 10 minutes to get to the airport. How many minutes early will
 1701 Toby be?
 1702
 1703 **Output of SFT-Intial Model:**
 1704 <think>
 1705 Okay, let's see. So the problem is about Toby reading a book and figuring out how early he'll be
 1706 at the airport. Hmm. Let me start by understanding each part step by step.
 1707
 1708 First, the book is 45 pages long. Each page averages 200 words. So, to find the total number of
 1709 words in the book, I need to multiply the number of pages by the average words per page. That
 1710 would be 45 pages times 200 words per page. Let me calculate that. 45 times 200... 45 times 200
 1711 is 9,000 words. So the book has 9,000 words in total.
 1712
 1713 Next, Toby's reading rate is 300 words per minute. So, to find out how long it takes him to read
 1714 the entire book, I need to divide the total number of words by his reading rate. That's 9,000
 1715 words divided by 300 words per minute. Let me do that division. 9,000 divided by 300. Hmm,
 1716 300 times 30 is 9,000. So that's 30 minutes. So Toby will take 30 minutes to read the book.
 1717
 1718 But wait, he has to be at the airport in 60 minutes, and it takes him 10 minutes to get there. **So**
 1719 **the total time he needs to leave his house is 60 minutes (time to be at the airport) plus 10 minutes**
 1720 **(travel time) which is 70 minutes.** But he only needs 30 minutes to read the book. So if he starts
 1721 reading now, he'll finish in 30 minutes. Then he has $70 - 30 = 40$ minutes left before he needs to
 1722 leave. Therefore, he'll be 40 minutes early.
 1723
 1724 Wait, but let me check again to make sure I didn't miss anything. Let me recap: Total words in
 1725 the book: $45 \text{ pages} * 200 \text{ words/page} = 9,000 \text{ words}$. Reading time: $9,000 \text{ words} / 300 \text{ words per}$
 1726 $= 30 \text{ minutes}$. Time needed to get to the airport: 10 minutes. Total time before he needs
 1727 to leave: 60 minutes.
 1728
 1729 So time he has after finishing reading: **$60 + 10 - 30 = 40$ minutes.** Therefore, he's 40 minutes
 1730 early. That seems right. I don't think I made any mistakes here. The key steps were calculating
 1731 the total words, then the reading time, and then subtracting that from the total time he has before
 1732 he needs to leave. Yeah, that makes sense.

1728 </think>
 1729
 1730 ...
 1731 ****Final Answer**:** \boxed{40}

1732 **Output of HSIR-DPO Model:**
 1733
 1734 <think>
 1735 Okay, let's see. Toby has a 45-page book to read. Each page averages 200 words. He reads at
 1736 300 words per minute. He has 60 minutes before he needs to be at the airport, and it takes him 10
 1737 minutes to get there. The question is how many minutes early he'll be if he reads the whole book
 1738 and leaves right after. Hmm, let me break this down step by step.
 1739 First, I need to figure out how many words are in the entire book. Since there are 45 pages and
 1740 each page has 200 words, I can multiply those two numbers. So 45 pages times 200 words per
 1741 page. Let me calculate that. 45 times 200... 45 times 200 is 9,000 words. So the book has 9,000
 1742 words total.
 1743 Next, Toby reads at a rate of 300 words per minute. To find out how long it takes him to read the
 1744 entire book, I need to divide the total number of words by his reading rate. That's 9,000 words
 1745 divided by 300 words per minute. Let me do that division. $9,000 \div 300$. Hmm, 300 times 30 is
 1746 9,000. So that's 30 minutes. So reading the book takes him 30 minutes.
 1747 But he has to get to the airport, which takes 10 minutes. So the total time from when he starts
 1748 reading until he leaves for the airport is the time reading plus the time to get there. That's 30
 1749 minutes + 10 minutes = 40 minutes. Wait, but he has 60 minutes before he needs to be at the
 1750 airport. **So if he finishes reading and leaves 40 minutes later, he'll have 60 - 40 = 20 minutes left.**
 1751 That means he'll be 20 minutes early.
 1752 Let me just verify each step again. Pages times words per page: $45 \times 200 = 9000$. Reading time:
 1753 $9000 / 300 = 30$. Time to airport: 10. Total time: $30 + 10 = 40$. Time left: $60 - 40 = 20$. Yep, that checks
 1754 out. **So the answer is 20 minutes early.**
 1755 </think>
 1756
 1757 ...
 1758 ****Final Answer**:** \boxed{20}

1759
 1760
D LLM USAGE
 1761

1762 During the paper writing, we used the proprietary LLMs as general-purpose assistants to polish some
 1763 sentences. We did not prompt them to generate research ideas or search for related works, thus
 1764 avoiding the risk of introducing false information. In the experiments, we instructed the DeepSeek-R1
 1765 to obtain the intermediate reasoning trajectories for the unlabeled MedQA training set. The detailed
 1766 prompt is shown in Table 6. The way of distilling reasoning trajectories from proprietary LLMs is
 1767 common in the community, and we believe that this behavior does not violate the policies.
 1768

1769
 1770
 1771
 1772
 1773
 1774
 1775
 1776
 1777
 1778
 1779
 1780
 1781